

## Proteomics- and Transcriptomics-Based Screening of Differentially Expressed Proteins and Genes in Brain of Wig Rat: A Model for Attention Deficit Hyperactivity Disorder (ADHD) Research

Misato Hirano,<sup>†</sup> Randeep Rakwal,<sup>\*,†</sup> Junko Shibato,<sup>†</sup> Hirofumi Sawa,<sup>‡</sup> Kazuo Nagashima,<sup>‡</sup> Yoko Ogawa,<sup>§</sup> Yasukazu Yoshida,<sup>§</sup> Hitoshi Iwahashi,<sup>§</sup> Etsuo Niki,<sup>§</sup> and Yoshinori Masuo<sup>†</sup>

Human Stress Signal Research Center (HSS), National Institute of Advanced Industrial Science and Technology (AIST), Tsukuba West, 16-1 Onogawa, Tsukuba 305-8569, Japan, Hokkaido University, Sapporo 060-8638, Japan, and HSS, AIST Kansai Center, 1-8-31, Midorigaoka, Ikeda 563-8577, Japan

Received January 12, 2008

Two global omics approaches were applied to develop an inventory of differentially expressed proteins and genes in Wig rat, a promising animal model of attention-deficit hyperactivity disorder (ADHD). The frontal cortex, striatum, and midbrain of Wig rat at 4 weeks of age were dissected for proteomics and transcriptomics analyses. Two-dimensional gel electrophoresis detected 13, 1, and 16 differentially expressed silver nitrate-stained spots in the frontal cortex, striatum, and midbrain, respectively. Peptide mass fingerprinting/tandem mass spectrometry identified 19 nonredundant proteins, belonging to 7 functional categories, namely, signal transduction, energy metabolism, cellular transport, protein with binding function, protein synthesis, cytoskeleton, and cell rescue. Interestingly, 10 proteins that were identified in the present study were also previously reported in studies involving neurodegenerative diseases and psychiatric disorders, such as Alzheimer's disease (AD), Parkinson's disease, and Schizophrenia. Moreover, some of the proteins identified in the midbrain were involved in synaptic vesicular transport, suggesting abnormality in neurotransmitter release in this region. On the other hand, transcriptomics analysis of combined frontal cortex, striatum, and midbrain by rat whole genome 44K DNA oligo microarray revealed highly up-regulated (28) and down-regulated (33) genes. Functional categorization of these genes showed cellular transport, metabolism, protein fate, signal transduction, and transcription as the major categories, with 26% genes of unknown function. Some of the identified genes were related to AD, fragile X syndrome, and ADHD. This is a first comprehensive study providing insight into molecular components in Wig rat brain, and will help to elucidate the roles of identified proteins and genes in Wig rat brain, hopefully leading to uncovering the pathogenesis of ADHD.

**Keywords:** Gel-based proteomics • Wig • ADHD • brain regions • biomarkers • neurodegenerative diseases

### 1. Introduction

Patients with attention-deficit hyperactivity disorder (ADHD) show motor hyperactivity under inappropriate situations, especially during childhood. A potential pathogenesis of ADHD results in abnormality in the development of dopamine (DA) neuron; however, the etiology of this developmental disorder is unknown (reviewed in ref 1). Various studies have focused on investigating the mechanism of ADHD using animal models (reviewed in refs 2 and 3). Wiggling (Wig) Wistar King Aptekman/Hokkaido (WKAH) rats were recently designated from a strain of the Long-Evans Cinnamon (LEC) as a new rat model of ADHD.<sup>4</sup> The Wig rats show motor abnormalities such as

"wiggling" movement, a kind of circular movement with head shaking induced by stimulation. This single detailed behavioral study revealed that Wig rats at 12–14 weeks of age show hyperactivity, impaired working memory and impulsive behavior, as demonstrated by motor activity and the open-field and Y-maze tests.<sup>4</sup> It was also reported that these abnormalities are transmitted by a single autosomal recessive gene with Mendelian pattern. These characteristics make the Wig rat a possible animal model of human ADHD.

With a model in place, the next logical step was to analyze it further, and for this, Wig rats at 4–5 weeks of age, the juvenile period, were used in the present study. The reason for selecting juvenile period (in rats) is correlated with the fact that ADHD patients are characterized by hyperactivity, which is most prominent during childhood. Moreover, in a rat model of ADHD where 6-hydroxydopamine (6-OHDA) was intracranially administered during the neonatal period, it was the juvenile rats that showed an increase in spontaneous motor

\* To whom correspondence should be addressed. Dr. Randeep Rakwal, HTRC, AIST, Tsukuba West, 16-1 Onogawa, Tsukuba 305-8569, Japan. E-mail, rakwal-68@aist.go.jp; fax, +81-29-861-8508.

<sup>†</sup> Human Stress Signal Research Center (HSS), National Institute of Advanced Industrial Science and Technology (AIST).

<sup>‡</sup> Hokkaido University.

<sup>§</sup> HSS, AIST Kansai Center.

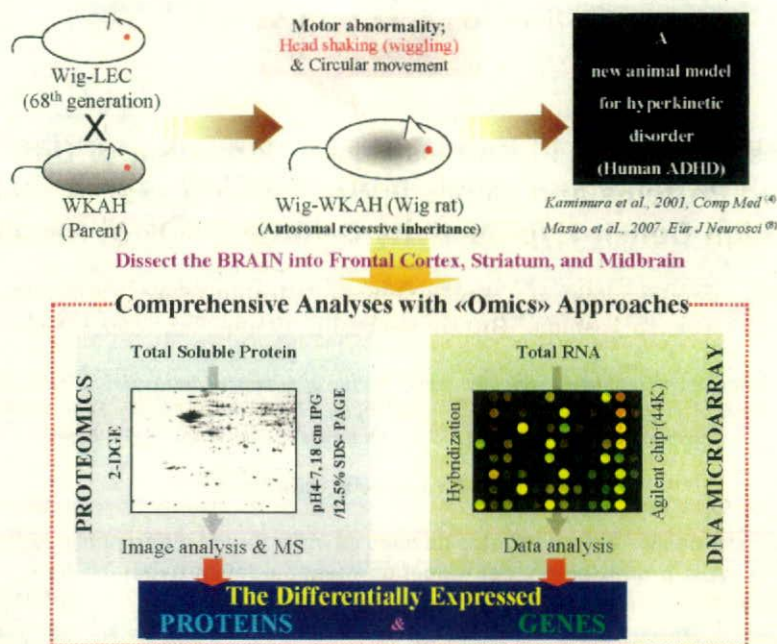


**Figure 1.** The Wig rat and a workflow representing the systematic omics approaches used for investigating the changes in protein and genes in the 3 dissected brain regions of Wig rat.

activity (SMA), which corresponds to preadolescence in humans.<sup>5-7</sup> Masuo and co-workers recently examined juvenile Wig rats, finding abnormalities in the SMA and development of DA neurons.<sup>8</sup> Moreover, when a cDNA macroarray (Atlas Rat 1.2, BD Biosciences Clontech) was used, changes in the expression of multiple genes, such as adenosine A2a receptor, macrophage migration inhibitory factor, and calbindin 2, were detected in 3 brain regions (frontal cortex, striatum, and midbrain) of these juvenile Wig rats over the control WKAH rats. These two studies preliminarily uncovered an aspect of Wig rat as an important animal model for ADHD, but further investigation is necessary to (1) uncover in greater detail the gene expressions at a global level using DNA microarray-based screening in these 3 regions, (2) look into the corresponding protein level changes, and (3) elucidate the mechanisms of the hyperactivity in Wig rat. Furthermore, it has been reported that the frontal cortex and ventral striatum, including the nucleus accumbens, may play crucial roles in ADHD.<sup>1,9</sup> We also separated the midbrain, since this region contains the substantia nigra and ventral tegmental area, regions rich in DA neurons.

To achieve this goal, we have selected two global "omics" approaches, namely, proteomics<sup>10-12</sup> and transcriptomics,<sup>13-15</sup> prominent and well-established technologies widely applied to address the biological questions in animals and other organisms. Our group has recently started focusing on gel-based (two-dimensional gel electrophoresis, 2-DGE) proteomics of the rat brain regions<sup>16</sup> with an aim to use this approach for a comprehensive investigation of stress-related protein profiling in the brain.<sup>16</sup> Moreover, our initial work in this direction has resulted in an improved protein extraction/solubilization protocol for brain proteomics.<sup>16</sup> This method involves the use of finely ground brain/brain regions in liquid nitrogen, before precipitating the total proteins with trichloroacetic acid (TCA)/acetone extraction buffer (TCAEB) followed by solubilization of proteins in lysis buffer (LB). On the other hand, DNA microarray analysis is routinely employed for unraveling the

genome-wide expression profiles and for screening of the genes of interest. The drawback is that this powerful genomic tool does not provide any direct information on protein levels and their state of modifications, mainly due to post-translation regulation, which results in a lack of correlation between mRNA and protein abundance.<sup>17</sup> As 2-DGE-based proteomics approach lacks wide coverage, it would be advantageous to employ a combination of proteomics and transcriptomics to any study where the identification of target molecular components (genes and proteins) is one of the goals (Figure 1).

Nevertheless, both these technologies are powerful screening methods for surveying the proteins and genes of interest in a particular sample, in our case, the Wig rat brain. In the present study, we have investigated the proteomes of precisely dissected frontal cortex, striatum and midbrain by 2-DGE in conjunction with peptide mass finger printing (PMF) methods (matrix-assisted laser desorption/ionization mass spectrometry, MALDI-TOF-MS), and tandem mass spectrometry by Q-TOF-MS/MS and nano electrospray ionization liquid chromatography-mass spectrometry (nESI-LC-MS/MS) for protein identifications. In parallel, DNA microarray analysis, along with reverse transcriptase-polymerase chain reaction (RT-PCR) experiments, was used to unravel the transcriptomes in these same brain regions.

## 2. Materials and Methods

**2.1. Growth Conditions and Dissection of Brain.** The experiments were carried out in accordance (Guidelines for the Care and Use of Laboratory Animals in the National Institute for Environmental Studies, Japan, and in the National Institute of Advanced Industrial Science and Technology, Japan) with the regional legal regulations. Male Wig and WKAH rats were housed in acrylic cage at 22 °C with tap water and laboratory chow *ad libitum*. The breeding rooms were illuminated from 07:00 to 19:00 h in 12 h cycles. The rats were decapitated at 4 weeks of age, whole brains were rapidly

removed, and whenever required, the frontal cortex, striatum, and midbrain were separated on ice.<sup>7,18</sup> For the midbrain, we made a frontal section between the anterior and posterior edges of the substantia nigra in order to investigate alterations in the region rich in dopaminergic neurons. On the other hand, the frontal cortex and striatum were dissected with the method of Glowinski and Iversen<sup>19</sup> with some modifications.<sup>16,19</sup> Each sample was immediately weighed, flash-frozen in liquid nitrogen, and stored at  $-80^{\circ}\text{C}$  until extraction of total crude protein.

**2.2. Extraction of Total Protein.** Extraction of total protein was performed using a two-step protein extraction protocol.<sup>16,20</sup> The three brain regions dissected from each rat were individually prepared for extraction of proteins. Briefly, frozen brain regions were separately placed in liquid nitrogen, and ground thoroughly to a very fine powder with a mortar and pestle. The tissue powder (ca. 50–100 mg) was transferred to sterile tubes containing cold TCAAEB (acetone containing 10% (w/v) TCA, and 0.07% mercaptoethanol), and the proteins were precipitated for 1 h at  $-20^{\circ}\text{C}$ , followed by centrifugation at 17 400g for 15 min at  $4^{\circ}\text{C}$ . The supernatant was decanted, and the pellet was washed twice with chilled wash buffer (acetone containing 0.07% mercaptoethanol, 2 mM EDTA, and two EDTA-free proteinase inhibitor cocktail tablets (Roche Diagnostics GmbH, Mannheim, Germany) in a final volume of 100 mL buffer), followed by removal of all the acetone. The pellet was subsequently solubilized in LB [7 M urea, 2 M thiourea, 4% (w/v) CHAPS, 18 mM Tris-HCl (pH 8.0), 14 mM Trizma base, two EDTA-free proteinase inhibitor cocktail tablets in a final volume of 100 mL buffer, and 0.2% (v/v) Triton X-100 (R), containing 50 mM dithiothreitol (DTT); hereafter called LB-TT], incubated for 20 min at  $4^{\circ}\text{C}$  with occasional vortexing, and centrifuged at 17 400g for 15 min at  $10^{\circ}\text{C}$ . In this experiment, a further purification/clean up of the solubilized protein samples was done by precipitating the supernatant at the last step with 4 vol of cold ( $-20^{\circ}\text{C}$ ) acetone followed by resolubilization in LB-TT as above. The supernatant was pooled from each sample set and was then used for protein determination by a Coomassie Plus (PIERCE, Rockford, IL) protein assay kit at room temperature (RT), and stored in aliquots at  $-80^{\circ}\text{C}$  till analyzed by 2-DGE.

**2.3. Two-Dimensional Gel Electrophoresis.** 2-DGE was carried out using IPG strip gels (GE Healthcare Bio-Sciences AB, Uppsala, Sweden) on an IPGphor unit (GE Healthcare) followed by the second dimension using 12.5% polyacrylamide gels (PAGs) on a Nihon Eido (Tokyo, Japan) sodium dodecyl sulfate-PAG electrophoresis (SDS-PAGE) vertical electrophoresis unit. The volume carrying 125  $\mu\text{g}$  of total soluble protein was mixed with LB-TT containing 0.5% (v/v) pH 4–7 IPG buffer to bring to a final volume of 350  $\mu\text{L}$ . A trace of bromophenol blue (BPB) was added and the whole mixture was kept at RT for 5 min, vortexed, and centrifuged at 17 400g for 15 min at  $10^{\circ}\text{C}$  followed by pipetting into a 18 cm strip holder tray. IPG strips (pH 4–7; 18 cm) were carefully placed onto the protein samples, covered with a lid, and placed into the IPGphor unit. The IPG strips were placed gel-face down onto the protein samples avoiding air bubbles and allowed to passively rehydrate with the protein samples for 1.5 h, followed by overlaying the IPG strips with 1000  $\mu\text{L}$  of cover fluid, and this was directly linked to a five-step active rehydration and focusing protocol (18 cm strip) as described previously.<sup>16</sup> The whole procedure was carried out at  $20^{\circ}\text{C}$ , and a total of 68 902 Vh was used for the 18 cm strip. Following IEF, the IPG strips were immediately used for the second dimension or stored at  $-20^{\circ}\text{C}$ .

The strip gels were incubated in equilibration buffer (50 mM Tris-HCl (pH 8.8), 6 M urea, 30% (v/v) glycerol, and 2% (w/v) SDS) containing 2% (w/v) DTT for 10 min (twice) with gentle agitation, followed by incubation in the same equilibration buffer supplemented with 2.5% (w/v) iodoacetamide twice at RT. Preceding the second-dimension separation, IPG strips were then rinsed with cathode running buffer [0.025 M Tris, 0.192 M glycine and 0.2% (w/v) SDS], placed onto polyacrylamide gels and overlaid with overlay agarose solution [60 mM Tris-HCl, pH 6.8, 60 mM SDS, 0.5% (w/v) agarose, and 0.01% (w/v) BPB]. The lower anode buffer contained 0.05 M diethanolamine and 0.05 M acetic acid. SDS-PAGE (4% T, 2.6% C stacking gels, pH 6.8, and 12.5% T, 2.6% C separating gels, pH 8.8) as the second dimension was carried out at constant current of 40 mA/per 18 cm gels for ca. 4.5 h. The % T is the total monomer concentration expressed in grams per 100 mL and % C is the percentage cross-linker. The stacking and separating gel buffer concentrations were 0.125 M Tris-HCl, pH 6.8, and 0.375 M Tris-HCl, pH 8.8, respectively. Molecular masses were determined by running standard protein markers (DualColor PrecisionPlus Protein Standard; Bio-Rad). For each sample, triplicate IPG strips and PAGs were processed for electrophoresis under the same conditions.

**2.4. Protein Visualization and Spot Quantitation.** To visualize the protein spots, the polyacrylamide gels were stained with silver nitrate (Plus One Silver Staining Kit Protein; GE Healthcare). Protein patterns in the gels were recorded as digitalized images using a digital scanner (CanoScan 8000F, resolution 300 dpi), and saved as TIFF files. The gels were quantitated in profile mode as instructed in the operating manual of the ImageMaster 2D Platinum software ver. 5.0 (GE Healthcare). To analyze differentially expressed spots, relative ratio of spot volume over the corresponding spot in control was calculated using the software. These results (spot differences) were also manually (visually) confirmed. Moreover, the silver nitrate stained spots were selected for comparative profiling only if they were confirmed in all three independent gel replications. Differentially expressed spots were defined as the ratio by more than 1.2-fold for increment or less than 0.8-fold for decrement in all three gel replications.<sup>20</sup> The differentially expressed spots were excised from the 2-D gels using a gel picker (One Touch Spot Picker, P2D1.5 and 3.0, The Gel Company, San Francisco, CA), and stored at  $-30^{\circ}\text{C}$ .

**2.5. MALDI-TOF-MS and Q-TOF-MS/MS.** Proteins were identified by PMF methods and tandem mass spectrometry.

**2.5.1. MALDI-TOF-MS.** In case of PMF, the excised gel spots were destained with 100  $\mu\text{L}$  of destain solution [30 mM potassium ferricyanide (Sigma-Aldrich, St. Louis, MO), in 100 mM sodium thiosulfate (Merck, Darmstadt, Germany)], with shaking for 5 min. After the solution was removed, the gel spots were incubated with 200 mM ammonium bicarbonate (Sigma; and hereafter called AMBIC) for 20 min. The gel pieces were dried in a speed vacuum concentrator for 5 min and then rehydrated with 20  $\mu\text{L}$  of 50 mM AMBIC containing 0.2  $\mu\text{g}$  of modified trypsin (Promega, Madison, WI) for 45 min on ice. After removal of solution, 30  $\mu\text{L}$  of 50 mM AMBIC was added and the digestion was performed overnight at  $37^{\circ}\text{C}$ . The peptides were desalted and concentrated using C18 nanoscale (porus C18) column (homemade). For the analysis of MALDI-TOF MS by PMF method, the peptides were eluted by 0.8  $\mu\text{L}$  of matrix solution [70% acetonitrile (Merck), 0.1% TFA (Merck), and 10 mg/mL  $\alpha$ -cyano-4-hydroxycinnamic acid (Sigma)]. The eluted peptides were spotted onto a stainless steel target plate.

Masses of peptides were determined using MALDI-TOF-MS (Model M@LDI-R; Micromass, Manchester, U.K.). Calibration was performed using internal mass of trypsin autodigestion product ( $m/z$  2211.105).

**2.5.2. Q-TOF-MS/MS.** For analyses by MS/MS, 15  $\mu$ L of the peptide solutions from the digestion supernatant (section 2.5.1) was diluted with 30  $\mu$ L in 5% formic acid, loaded onto the column, and washed with 30  $\mu$ L of 5% formic acid. Peptides were eluted with 2  $\mu$ L methanol/H<sub>2</sub>O/formic acid (50/49/1, v/v/v) directly into precoated borosilicate nanoelectrospray needles (EconoTip, New Objective). MS/MS of peptides generated by in-gel digestion was performed by nano-ESI on a Q-TOF2 MS (Micromass). The source temperature was 80 °C. A potential of 1 kV was applied to the precoated borosilicate nanoelectrospray needles in the ion source combined with a nitrogen backpressure of 0–5 psi to produce a stable flow rate (10–30 nL/min). The mass spectrometer was operated in an automatic data-dependent MS/MS to collect ion signals from the eluted peptides. In this mode, the most abundant peptide ion peak with doubly or triply charged ion in a full scan mass spectrum ( $m/z$  400–1500) was selected as the precursor ion. Finally, an MS/MS spectrum was recorded to confirm the sequence of the precursor ion using collision-induced dissociation (CID) with a relative collision energy dependent on molecular weight. The cone voltage was 40 V. The quadrupole analyzer was used to select precursor ions for fragmentation in the hexapole collision cell. The collision gas was Ar at a pressure of  $(6 \sim 7) \times 10^{-5}$  mbar and the collision energy was 20–30 V. Product ions were analyzed using an orthogonal TOF analyzer, fitted with a reflector, a microchannel plate detector and a time-to-digital converter. The data were processed using a MassLynx (Ver. 3.5) Windows NT PC system.

**2.5.3. Protein Identification.** Protein identification was performed by searching the National Center for Biotechnology Information (NCBI) nonredundant database using the MASCOT search engine (Matrix Science, Inc., London, U.K.; www.matrixscience.com), which uses a probability-based scoring system.<sup>21</sup> The following parameters were used for database searches with MALDI-TOF PMF data: monoisotopic mass, 50 ppm mass accuracy, trypsin as digesting enzyme with 1 missed cleavage allowed, carbamidomethylation of cysteine as a fixed modification, oxidation of methionine, N-terminal pyroglutamic acid from glutamic acid or glutamine as allowable variable modifications. For database searches with MS/MS spectra, the following parameters were used: average mass; 1.0 Da peptide and MS/MS mass tolerance; peptide charge of +1, +2, or +3; trypsin as digesting enzyme with 1 missed cleavage allowed; carbamidomethylation of cysteine as a fixed modification; oxidation of methionine as allowable variable modifications. Taxonomy was limited to mammalia for both MALDI and MS/MS ion searches. For MALDI-TOF-MS data to qualify as a positive identification, a protein's score had to equal or exceed the minimum significant score. Positive identification of proteins by MS/MS analysis required a minimum of two unique peptides, with at least one peptide having a significant ion score. The identified peptides are listed in Supplementary Table 1.

**2.6. nESI-LC-MS/MS.** Differentially expressed protein spots were digested with sequencing-grade modified trypsin according to a previous procedure<sup>22</sup> with minor modifications. Briefly, protein spots were washed twice with 100 mM AMBIC and then dehydrated with acetonitrile. The gel pieces were reduced with

10 mM DTT at 56 °C for 45 min and alkylated with 50 mM iodoacetamide for 45 min at RT in the dark in AMBIC solution. Gel pieces were washed with 20 mM AMBIC, dehydrated with acetonitrile, and air-dried. Gel pieces were subjected to in-gel trypsin digestion with 30  $\mu$ L of 20 mM AMBIC containing 15 ng/ $\mu$ L sequence-grade modified trypsin (17 000 U/mg; Promega) at 37 °C for 18 h. The peptides were extracted from the gel pieces twice with 20  $\mu$ L of 20 mM AMBIC and three times with 20  $\mu$ L of 0.5% trifluoroacetic acid (TFA) in 50% acetonitrile. The peptides extracted in the five steps were combined together and concentrated to 20  $\mu$ L by using a centrifugal concentrator (CC-105; TOMY, Tokyo, Japan). The peptides in 20  $\mu$ L were used for mass spectral analysis on a LCQ Deca linear ion trap mass spectrometer (nESI-LC-MS/MS; Thermo Electron, Waltham, MA) through a nanoelectrospray ionization source. Briefly, online capillary LC included a monolithic reverse-phase trap column (0.2 mm  $\times$  5 cm, MonoCap for fast-flow, GL Science, Tokyo, Japan) and a fast-equilibrating C18 capillary column (monolith-type column; i.d., 0.1 mm; length, 50 mm; GL Science). Sample was loaded onto peptide traps for concentration and desalting prior to final separation by C18 column using a linear acetonitrile gradient ranging from 5% to 65% solvent B [H<sub>2</sub>O/acetonitrile/formic acid, 10/90/0.1 (v/v)] in solvent A [H<sub>2</sub>O/acetonitrile/formic acid, 98/2/0.1 (v/v)] for a duration of 40 min. The mass/charge ( $m/z$ ) ratios of eluted peptides and fragmented ions from fused-silica Fortis Tip emitter (150  $\mu$ M o.d., 20  $\mu$ M i.d.; AMR, Inc., Tokyo, Japan) were analyzed in the data-dependent positive acquisition mode on LC-MS/MS. Dynamic exclusion used was repeat count (2), repeat duration (0.5 min), exclusion list size (25), and exclusion duration (3.0 min). Following each full scan ( $m/z$  400–2000), a data-dependent triggered MS/MS scan for the most intense parent ion was acquired. The heated fused-silica Fortis Tip emitter was held at ion sprays of 1.8 kV and a flow rate of 300 nL/min.

Acquired LC-MS/MS data were submitted to a local MASCOT (version 2.1) server for querying all MS/MS ion search against NCBI nr (Rat Protein Database, update 2006.09.09). The typical parameters used in the MASCOT MS/MS ion search were maximum of one trypsin miss cleavage, fixed modification of cysteine carbamidomethylation, variable modification of methionine oxidation, peptide mass tolerance of  $\pm 2$  Da, threshold ( $p < 0.05$ ), minimum ion counts (0), and fragment mass tolerance of  $\pm 0.8$  Da. Criteria applied for unambiguous assignments of all proteins were a minimum of two nonredundant peptides with a score higher than 39. The identified peptides are listed in Supplementary Table 1.

**2.7. 1-DGE, Subcellular Fractionation, and Western Analysis.** Proteins were fractionated from tissue powder (ca. 50–100 mg) of the brain regions using the ProteoExtract Subcellular Proteome Extraction Kit (EMD Chemicals, Inc., Darmstadt, Germany) as per the instructions provided along with the kit. Soluble protein samples of each fraction were further purified using the 2-D Clean-Up Kit (GE Healthcare) and resolubilized in LB-TT. Proteins in the supernatant were quantified using Coomassie Plus protein assay kit, and stored in aliquots at  $-80$  °C until analyzed. Prior to SDS-PAGE, 50  $\mu$ L of each fractionated protein sample was mixed with 20  $\mu$ L of SDS sample buffer [62 mM Tris (pH 6.8), 10% (v/v) glycerol, 2.5% (w/v) SDS, and 5% (v/v) 2-mercaptoethanol] and a drop of BPB. After incubation on the bench (ambient RT of 25 °C) for 10 min, the mixture was centrifuged, and a total of 5  $\mu$ g of

**Table 1.** Primer Combinations Used for RT-PCR of Genes Encoding the Changed Proteins Identified by 2-DGE Analysis

accession (gene)	spot number <sup>a</sup>	forward primer		reverse primer		product size (bp)	number of cycles
		primer name	nucleotide sequence (5'-3')	primer name	nucleotide sequence (5'-3')		
NM_031603.1	6, 55, 77	RB091	CGATGGTGAAGAGCAGAATAAA	RB092	GGGACCAGTAAAAATCCACAGAA	300	22
BC085120	8, 10, 45, 46, 47	RB103	CTTGCTGTACGAAACAGCACTC	RB104	GTTTCATGCCACACAGATGTT	320	20
Z46882.1	13, 14	RB107	GCTCAGATTGACGACAACATTC	RB108	TCATGACTGTGTAGGGACTTGG	304	35
AF389425.1	15, 16	RB109	AAGATCATGCTGGAAGATGGTAA	RB110	AGACTAAATCCCAGCTGATGGA	269	33
XM_215069.3	19	RB111	CCCAGGTTTATATCCTCAGCAA	RB112	TCAGCTCCATTTGATGTTCTTG	299	25
AB027144.1	21, 22	RB113	AGCAGATGACCAGCAAACCTCAC	RB114	GGTCAGCACCAATTTCTGTAGTG	295	35
NM_021774.1	26	RB119	TGAATAGGAAACCCGTTGTACC	RB120	GCTGGTGAGTCTCTCTTCTC	310	28
X54531.1	49	RB135	AGCCAGTGAGACTGAGGAGAAC	RB136	CTCCTTCAGTGCGTGGTACATA	307	30
XM_342542.2	50	RB137	AAAGATCCAGACTGCTTCAAGG	RB138	ACTGGTCTCACTGTGTGGAAGA	296	30
NM_022402.1	54	RB117	TGCAGCTGATAAAGACTGGAGA	RB118	CCAGTGGGAGGTGTAGTCAGT	312	22
NM_013011.2	56, 57, 58	RB145	GCCCTCAACTTCTCTGTGTCT	RB146	AGCATGGATGACAAATGGTCTA	294	20
X66974.1	61	RB147	AGAGTTCAATGCCATCTTACA	RB148	GTTTCAAGAGAGTCAGGGCAGT	297	25
BC065582	62	RB149	CCATCGTCTATGAACTGGACAA	RB150	TGCCGGGGATAAAAATACTAAAA	295	25
NM_017236.1	74	RB163	GGGAGTTCTCAGTTGTGCTAGG	RB164	GAATGCAATGCCCTTTATTTGT	307	22
XM_575249.1	75	RB089	TCCAGCATTTACTGACTCCAGA	RB090	TGGCTGGCTTATTTACAACAAA	316	30
BC088850.1	79	RB169	GACACGCTGAAGAAGCTGAATA	RB170	GTGGAGCTTGCATGTGAACCTTA	295	25
BC098897.1	82	RB175	TCAGTTATCGCACTCGAGAAGA	RB176	CGCCCATCCATCTAATACTCTC	303	25
XM_574007.2	101	RB179	CTGAATTCCTGGACATCATCAA	RB180	CAAAGGGACAGCCAGTTCTACT	299	33

<sup>a</sup> Spot numbers correspond to the numbers indicated in Figures 1 and 2.

protein was loaded per sample/well. 1-DGE was carried out using 12.5% PAGs at constant current of 40 mA for ca. 3 h. The running buffer was composed of 0.025 M Tris, 0.192 M glycine, and 0.2% (w/v) SDS.

Electrotransfer of proteins on 1-D gel to a polyvinylidene difluoride (PVDF) membrane (NT-31, 0.45  $\mu$ m pore size; Nihon Eido) was carried out at 1 mA/cm<sup>2</sup> for 80 min using a semidry blotter (Nihon Eido) as described.<sup>23</sup> The anti-heat shock protein (HSP) 90 monoclonal antibody was commercially obtained from Abcam Ltd. (Cambridgeshire, U.K.). The ECL+plus Western Blotting Detection System protocol for blocking, primary and secondary antibody (anti-Rat IgG-H&L, Horseradish peroxidase linked whole antibody; from rabbit) incubation was followed exactly as described (GE Healthcare, Little Chalfont, Buckinghamshire, U.K.). Immunoassayed proteins were visualized on an X-ray film (X-OMAT AR, Kodak, Tokyo, Japan) using an enhanced chemiluminescence protocol according to the manufacturer's directions.

**2.8. RT-PCR.** Total RNA was isolated from ca. 50–100 mg of brain tissues using QIAGEN RNeasy Mini Kit (QIAGEN, MD). The quality of RNA is the single most important factor in determining the outcome of any transcriptomics analysis, and for this, the yield and RNA purity were determined spectrophotometrically (NanoDrop, Wilmington, DE) and visually confirmed using formaldehyde-agarose gel electrophoresis. Briefly, total RNA samples were DNase-treated with an RNase-free DNase (Stratagene, La Jolla, CA) prior to RT-PCR. First-strand cDNA was synthesized in a 50  $\mu$ L reaction mixture with a StartaScript RT-PCR Kit (Stratagene) according to the protocol provided by the manufacturer, using 10  $\mu$ g of total RNA isolated from frontal cortex, striatum and midbrain of Wig rat and control. The 50  $\mu$ L reaction mixture (in 1 $\times$  buffer recommended by the manufacturer of the polymerase) contained 1.0  $\mu$ L of the first-strand cDNA from above, 200 mM dNTPs, 10 pmol of each primer set, and 0.5 U of Taq polymerase (TaKaRa Ex Taq Hot Start Version, TaKaRa Shuzo, Shiga, Japan). Specific primers were designed from the 3'-UTR regions (forward and

reverse primer sequences are provided in Table 1) of each of the genes used in this study by comparison and alignment with all available related genes in the databases, NCBI. Thermal-cycling parameters were as follows: after an initial denaturation at 97  $^{\circ}$ C for 5 min, samples were subjected to a cycling regime of 20–35 cycles at 95  $^{\circ}$ C for 45 s, 55  $^{\circ}$ C for 45 s, and 72  $^{\circ}$ C for 1 min. At the end of the final cycle, an additional extension step was carried out for 10 min at 72  $^{\circ}$ C (TaKaRa PCR Thermal Cycle Dice, Model TP600, TaKaRa, Tokyo, Japan). After completion of the PCR, the total reaction mixture was mixed with 2.0  $\mu$ L of 10 $\times$  loading buffer and vortexed, 10  $\mu$ L of the mixture was loaded into wells of a 1.5% agarose (Agarose ME, Iwai Chemicals, Tokyo, Japan) gel, and electrophoresis was performed for ca. 30 min at 100 V in 1 $\times$  TAE buffer, using a Mupidex electrophoresis system (ADVANCE, Tokyo, Japan). The gels were stained (20  $\mu$ L of 50 mg/mL Ethidium bromide in 100 mL 1 $\times$  TAE buffer) for ca. 10 min, and the stained bands were visualized using an UV-transilluminator (ATTO, Tokyo, Japan).

**2.9. Transcriptomics Analysis and Validatory RT-PCR.** A rat 44K whole genome oligo DNA microarray chip (G4131A, Agilent Technologies, Palo Alto, CA) was used for the microarray experiment. Total RNA from each (150 ng) of the 3 brain regions (frontal cortex, striatum and midbrain) was pooled together into one master total RNA mix (450 ng), and labeled with Cy-3 or Cy-5 using an Agilent Low RNA Input Fluorescent Linear Amplification Kit (Agilent). Fluorescently labeled targets of control and Wig samples were hybridized to the same microarray slide with 60-mer probes. A flip labeling (dye-swap or reverse labeling with Cy3 and Cy5 dyes) procedure was followed to nullify the dye bias associated with unequal incorporation of the two Cy dyes into cDNA.<sup>24–26</sup> In our experience, the use of a dye-swap approach<sup>27</sup> provides a very stringent selection condition for changed genes rather than simply doing 2 or 3 replicates, which overlook the dye bias. The design of the microarray experiment is presented in Table 2. Hybridization and wash processes were performed according to the manufacturer's instructions, and hybridized microarrays were scanned using an Agilent Microarray scanner G2565BA.

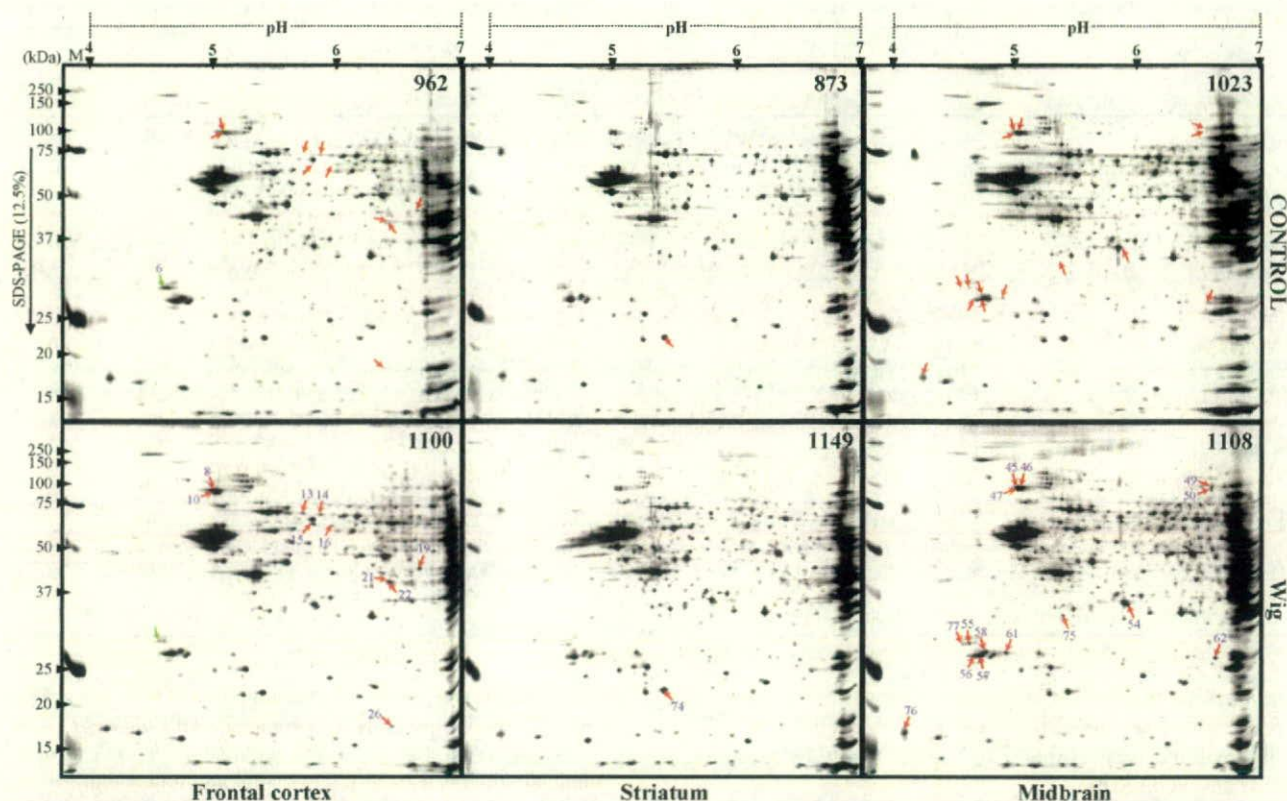


**Figure 2.** The 2-D gel protein profiles of Wig rat brain proteins. From left to right: frontal cortex, striatum, and midbrain. Proteins (ca. 125  $\mu$ g) were focused on precast IPG strips (18 cm, pH 4–7) in the first dimension; followed by separation on 12.5% SDS-PAGE in the second dimension. The proteins were stained with silver nitrate, and image analysis was performed using the ImageMaster software. Isoelectric points (pI) and molecular mass standards (M, Precision Plus Protein Standards, Bio-Rad) are indicated on the top and the left-hand side, respectively. The numbers of detected spots in each gel by the software are given at the top right-hand corners. Differentially expressed protein spots in each of the three brain regions as compared with respective controls are marked by arrows and numbers, and were taken for MS (MALDI-TOF-MS and Q-TOF-MS/MS) analyses. Red arrows show induced spots and green arrows show suppressed spots, respectively, over the controls.

**Table 2.** Details of Microarray Experiment

replicate <sup>a</sup>	sample	microarray slide no.	labeling	
			Cy3	Cy5
Pooled	BRAIN <sup>b</sup>	MA 1	Control	Wig
Biological		MA 2	Wig	Control
Replicates ( $\times 3$ )		RT-PCR validation <sup>c</sup>		

<sup>a</sup> Total RNA isolated from individual rat brain regions was used for cDNA synthesis. <sup>b</sup> Pooled three regions: frontal cortex, striatum, and midbrain. <sup>c</sup> For RT-PCR validation, total RNA from each region was analyzed separately over the control.

For detection of significant differentially expressed genes between control and Wig samples, each slide image was processed by Agilent Feature Extraction ver.8.1.1.1. This software measured Cy3 and Cy5 signal intensities of whole probes. Dye-bias tends to be a signal intensity-dependent; therefore, this software selected a probe set by rank consistency filter for dye-normalization, and the normalization was done by LOW-ESS (locally weighted linear regression) and it calculated log ratio of dye-normalized Cy3- and Cy5-signal, and final error of log ratio and significant value (*P*-value) based on propagate error model and universal error model. In this analysis, the threshold of significant differentially expressed genes determined *p*-value < 0.01 for the confidence that the feature is not

differentially expressed. In addition, erroneous data generated due to artifacts were eliminated before data analysis. Confirmatory RT-PCR was performed (see section 2.8) using 3'-UTR specific gene primers, which are listed in Table 3.

### 3. Results and Discussion

**3.1. 2-DGE and MS Identify 19 Nonredundant Proteins.** To investigate the alterations of protein profiles in the frontal cortex, striatum and midbrain of Wig rats over control WKAH rats, 2-DGE analysis of total soluble proteins from pooled three replicates was performed using 18 cm IPG strip format and 12.5% homogeneous SDS-PAGE. The representative 2-D gels stained with silver nitrate are shown in Figures 2 and 3. On 2-D gels of the three regions from Wig rats and controls, ca. 1000 spots in pH 4–7 range and 500 spots in pH 6–9 range were counted using the 2D ImageMaster software. To assess changes in protein profiles, relative ratio of spot volume was calculated using the software and changed (increased or decreased in Wig rat over control) spots were selected as mentioned in Materials and Methods. In Figure 4, average ratio of the selected spots in 3 independent gel replications is shown. In the frontal cortex, 11 spots (nos. 6, 8, 10, 13–16, 19, 21, 22, and 26) in pH 4–7 range and two spots (nos. 79 and 82) in pH 6–9 range were differentially expressed over control. In the striatum, one spot (no. 74) in pH 4–7 range and no spots in

**Table 3.** Primer combinations Used for Validatory RT-PCR of Genes Differential Expressed during Microarray Experiment

accession (gene)	forward primer		reverse primer		product size (bp)
	primer name	nucleotide sequence (5'-3')	primer name	nucleotide sequence (5'-3')	
XM_216315	RB319	GGCTGTGACATCTATCCCATCT	RB320	GTAACTTTGCCGACATCTTCC	295
NM_031703	RB321	GATCAGITCATAGGCACAGCAG	RB322	GTACACGAAGACACCACCAATG	297
NM_001014089	RB323	CCTGGCTAGGTTGTCCCTAAT	RB324	GATACCTGAATGGCACTTCTCTC	299
WIG_2007-1	RB325	<i>under patent application process</i>	RB326	<i>under patent application process</i>	302
XR_008769	RB331	AGTCGCGGATCCTGAAAGTAT	RB332	TTCATGATGATAGCCTCCTCTCT	315
XM_001067936	RB333	GCCAAGTCCATAAAACAAAGGA	RB334	GGGCTGTAGTAAAAATCCAGA	303
WIG_2007-2	RB301	<i>under patent application process</i>	RB302	<i>under patent application process</i>	303
EF125690	RB303	CTGTTTCCACCACACATTCTCTA	RB304	ATCAATGTCAGTTACCGTGCTG	303
NM_001013210.1	RB305	TAGAGGACTACTGGCTGCTCT	RB306	GGCCAAAGCTGTTAAGGAATAA	302
XM_001062086	RB307	CAGAAAACCCAAAAGGAAGATG	RB308	AGCCTTTGCTTTTTTCAGTCAAC	310
NM_001009713	RB309	TTTTACGGCTACATCGTCACAC	RB310	CCGAAAGAGGAAGTGAGATTA	308
XM_224672	RB311	ACATCAGCCAACACCTAATCCT	RB312	CTGTTTTACAGGACAAACTGG	302
XM_001080810	RB313	AAAATCCTCTGGCCTCTCTCTAC	RB314	ATCTAGGAGCATGAAAGCCTTG	301
NM_001000282	RB315	AGCCTTTCCTGCTCTAACATTG	RB316	TTCAGCATGGGAATCACAATAC	302
NM_001005888	RB317	AAATCTTCAGCTGACTGCCTTC	RB318	TGACATCTTGCATTCCAGACT	301

pH 6–9 range were differentially expressed over control. In the midbrain, 15 spots (nos. 45–47, 49, 50, 54–58, 61, 62, and 75–77) in pH 4–7 range and one spot (no. 101) in pH 6–9 range were differentially expressed over control. A total of 30 protein spots were analyzed by MALDI-TOF/Q-TOF MS (pH 4–7 range spots) and nESI-LC-MS/MS (spots in the pH range 6–9). From these, 19 nonredundant proteins were identified (Table 4).

**3.2. RT-PCR Analysis of Corresponding Gene Expression.** We also investigated whether these proteins are regulated at the mRNA level. The 3'-UTR specific primers of corresponding gene

(cDNA) sequences were designed (Table 1) and used those for checking the transcript levels using RT-PCR (Figure 5). Corresponding protein spot numbers are given on the left-hand side of the individual gel images, respectively. RT-PCR results reveal the corresponding mRNA levels in the frontal cortex, striatum, and midbrain of 4-week-old Wig rat. For spots 6, 55, and 77; 13 and 14; 15 and 16; 19, 26, 49, 82, and 101, the alteration of mRNA levels was in parallel with that of protein spot levels in the brain region from which the protein spot was identified. For spot 101, alteration of mRNA level was in parallel with that of protein spot level in all the 3 brain regions. However, in many

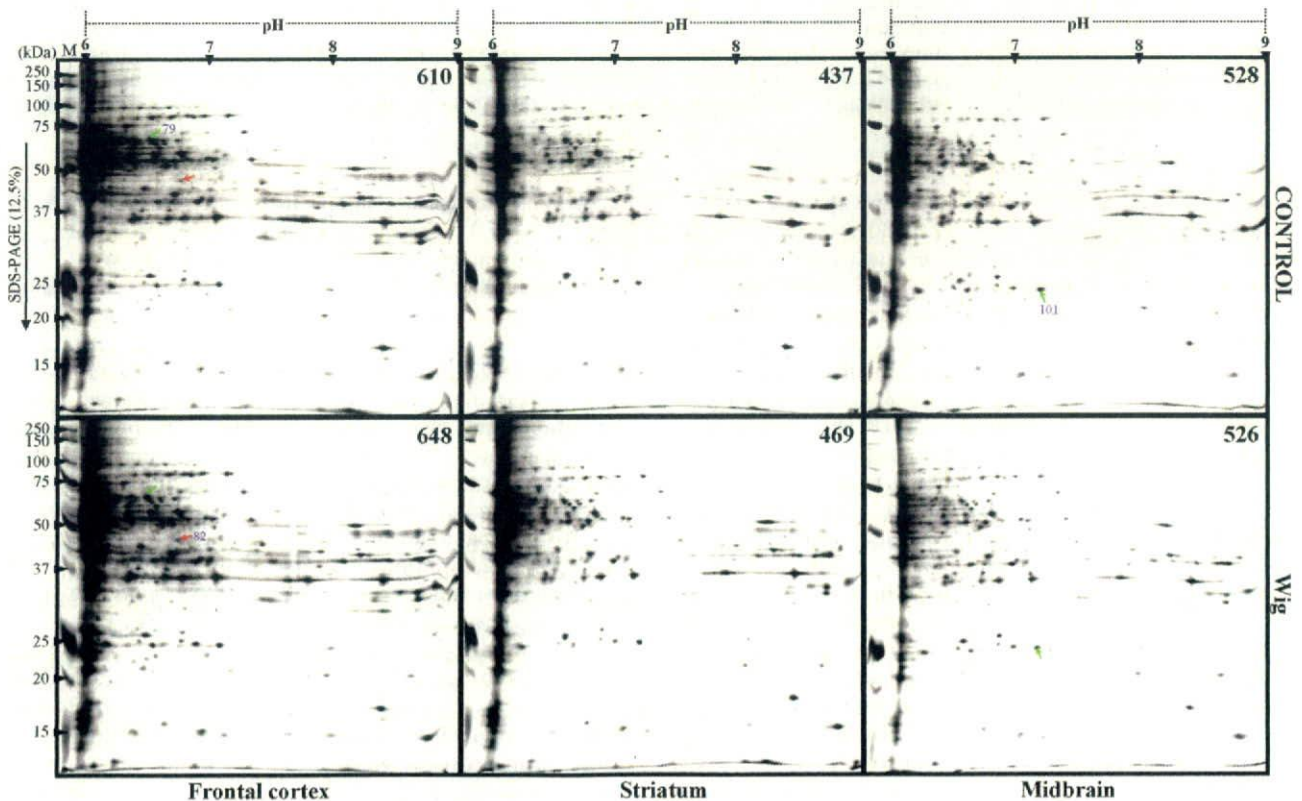


**Figure 3.** Silver nitrate stained 2-D gel basic protein profiles of frontal cortex, striatum, and midbrain. For separating proteins in the basic regions, pH 6–9 IPG strips (18 cm) was used. 2-DGE, image analysis, and spot markings are the same as in Figure 2.

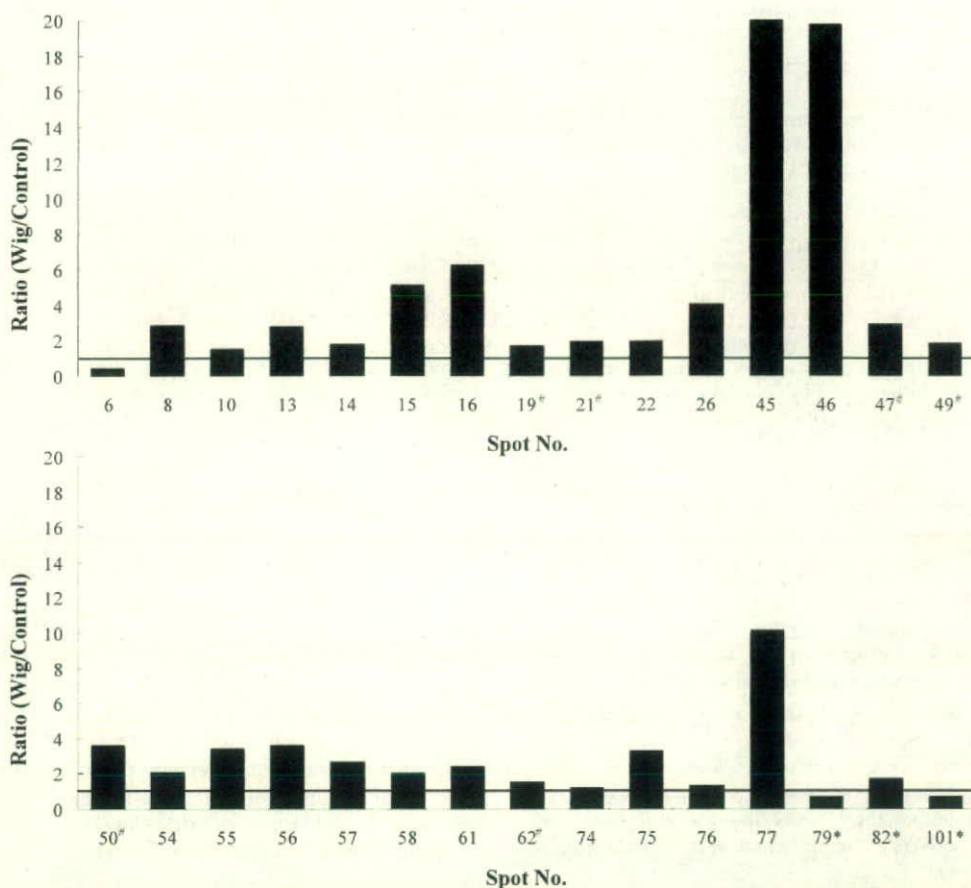


**Figure 4.** Graphical presentation of the differentially expressed protein spot volumes on 2-D gels of Wig rat frontal cortex, striatum, and midbrain. The corresponding spot numbers are the same as marked in Figures 2 and 3. The ratio (protein spots in Wig over control) of the differentially expressed spot volume was calculated using ImageMaster software. The volume of the corresponding spots in three gel replications altered more than 1.2-fold or less than 0.8-fold. Asterisks (\*) indicate the protein spots marked in Figure 3. Sharps (#) indicate spots which were detected in just two gel replications of three gel replications. Horizontal line indicates 1.0-fold.

cases, there was no correlation between mRNA levels and protein spot levels, suggesting possibilities of the time-lag between transcription and translation and/or the occurrence of post-translational modification.

**3.3. Functional Categorization and Subcellular Localization of Identified Proteins.** The identified proteins were classified into seven functional categories (Figure 6A), namely, signal transduction (26.3%), energy metabolism (26.3%), cellular transport (15.8%), protein with binding function (10.5%), protein synthesis (10.5%), cell division/cytoskeleton (5.3%), and protein fate (5.3%). The functional categories were determined using NCBI database or Rat Genome Database (RGD, <http://rgd.mcw.edu/>). Use of a subcellular localization tool (PSORT II, <http://psort.nibb.ac.jp/>) revealed that 15 (78.9%) out of 19 proteins were cytoplasmic in nature, whereas three proteins were localized in the nucleus and one protein was extracellular (Figure 6B). In the following subsections, we will discuss the identified proteins based on their functional categories.

**3.3.1. Signal Transduction.** In the signal transduction category, 5 proteins showed changed expressions. The 14-3-3 proteins (spots 6, 55, and 77; epsilon isoform, spots 56–58; zeta isoform) have 7 isoforms and are mainly localized to the synapses and neuronal cytoplasm.<sup>28</sup> The 14-3-3 isoforms interact with phosphoserine motifs on many proteins as

kinases, phosphatases, apoptosis-related proteins, and so forth.<sup>29</sup> Several reports have hinted at a possible relevance of 14-3-3 protein isoforms in neurological diseases.<sup>28–30</sup> Two reports have shown that the 14-3-3 zeta isoform is associated with tau protein, which is the main component of neurofibrillary tangles (NFTs), and an effector of tau phosphorylation on NFTs of Alzheimer's disease (AD).<sup>31</sup> It has also been reported that expression changes of the 14-3-3 epsilon protein might reflect impaired signaling and apoptosis in the brain regions of AD patients.<sup>29</sup> Our results reveal the induction of epsilon and zeta isoforms of 14-3-3 proteins in midbrain of Wig rats but a reduction in the epsilon isoform in the frontal cortex. It is possible that these derangements may be the cause of impaired signal transduction in the brain regions.

Dihydropyrimidase-related protein (DRP) 2 (spots 13 and 14) and collapsin response mediator protein (CRMP) 4 (spots 15 and 16) are members of cytosolic phosphoproteins that are involved in the signal transduction of semaphorin 3A leading to growth cone collapse. The activity and binding of DRP2, also known as CRMP2, are regulated via phosphorylation by glycogen synthase kinase 3 beta (GSK3b).<sup>32</sup> CRMP2 mediates the intracellular response to collapsin 1/semaphorin 3A, a repulsive extracellular guidance for axonal outgrowth, and is also involved in microtubule assembly.<sup>33</sup> Several reports have shown



**Table 4.** List of Identified Brain Proteins by Tandem Mass Spectrometry<sup>a</sup>

spot no	brain regions	MW (kDa)/pI observed	protein name	MW (da)/pI theoretical	method	accession	score	sequence coverage	subcellular localization
<i>Signal Transduction</i>									
6		29/4.5					89	27%	
55	FC and MB	28/4.6	<b>Chain A, 14-3-3 Protein Epsilon</b>	26912/4.92	MALDI-TOF	2BR9_A (NP_113791)	99	29%	Cytoplasm
77		27/4.5					129	35%	
13	FC	64/5.7	<b>Dihydropyrimidinase related protein-2 (DRP-2)</b>	62622/5.95	MALDI-TOF	XP_858120 (AAB07042)	147	31%	Cytoplasm
14		64/5.8					205	31%	Cytoplasm
15	FC	60/5.8	Collapsin response mediator protein 4 (CRMP4)	62327/6.04	MALDI-TOF	AAK64497			
16		59/5.9					112	42%	Nuclear
56		26/4.6					138	63%	Cytoplasm
57	MB	26/4.7	<b>14-3-3 Protein Zeta</b>	27879/4.72	MALDI-TOF	BAA11751 (NP_037143)			
58		27/4.7							
74	ST	19/5.4	<b>Phosphatidylethanolamine binding protein</b>	20902/5.48	MALDI-TOF	NP_058932			
<i>Energy Metabolism</i>									
26	FC	17/6.4	Fragile histidine triad protein (Fhit)	17394/6.16	MALDI-TOF	AAC23967 (NP_068542)	77	62%	Cytoplasm
50	MB	92/6.6	<b>Brain glycogen phosphorylase</b>	97361/6.31	MALDI-TOF	XP_342543	277	32%	Cytoplasm
62	MB	26/6.6	<b>Phosphoglycerate mutase 1 (PGM1)</b>	28900/6.67	MALDI-TOF	AAH53356 (NP_445742)	131	47%	Cytoplasm
101	MB	25/7.1	<b>Triosephosphate isomerase (Tpi) 1 protein</b>	27214/7.07	ESI-MS/MS	AAH61781	215	50%	Cytoplasm
82	FC	48/6.8	Pyruvate dehydrogenase E1 alpha 1	43872/8.35	ESI-MS/MS	AAH98897	143	25%	Cytoplasm, Mitochondria
<i>Cellular Transport</i>									
49	MB	98/6.6	<b>D100 (Dynamin 1)</b>	96209/6.32	MALDI-TOF	CAA38397	127	17%	Nuclear
75	MB	34/5.4	N-ethylmaleimide sensitive fusion protein attachment protein (SNAP)-beta	33850/5.32	MALDI-TOF	XP_534322 (XP_575249)	287	76%	Cytoplasm
79	FC	64/6.5	Syntaxin binding protein 1	67925/6.49	ESI-MS/MS	BAA32486 (AAH88850)	163	16%	Nuclear
<i>Protein with Binding Function</i>									
61	MB	27/4.9	Calbindin 2 (Calretinin)	31467/4.94	MALDI-TOF	AAH17646 (CAA47385)	110	32%	Cytoplasm
76	MB	17/4.0	Solution structure of calcium-calmodulin N-terminal domain	8483/3.90	Q-TOF	IJ70_A (NP_114175)	38	17%	Cytoplasm
<i>Protein Synthesis</i>									
19	FC	45/6.7	Tu translation elongation factor (EF-Tu)	56609/8.50	MALDI-TOF	XP_215069	149	29%	Extracellular, including cell wall
54	MB	37/5.9	Acidic ribosomal phosphoprotein PO	32527/5.28	MALDI-TOF	AAB65436 (NP_071797)	128	38%	Cytoplasm
<i>Cell Division/Cytoskeleton</i>									
21	FC	42/6.4	<b>CDCrel-1A1</b>	42487/6.21	MALDI-TOF	BAB87114	194	40%	Cytoplasm
22		41/6.4							
<i>Cell Rescue</i>									
8		86/5.0					145	24%	
10		82/5.0					174	25%	
45	FC and MB	98/5.0	<b>Heat shock protein HSP 90-alpha</b>	83445/5.00	MALDI-TOF	Q9GKX7 (NP_786937)			
46		98/5.0							
47		94/5.0							

<sup>a</sup> Identified proteins were classified into functional categories. The altered proteins (>1.2-fold for increment or <0.8-fold for decrement) in the frontal cortex, striatum, and midbrain of Wistar rats were identified using MALDI-TOF, Q-TOF, or LC-ESI-MS/MS. Differentially expressed spots in different brain regions are abbreviated as FC, frontal cortex; MB, midbrain; and ST, striatum. Bold letters indicate proteins reported to be involved in neurodegenerative diseases (e.g. Alzheimer's and Parkinson's disease, Schizophrenia) and mental disorders. Accession numbers in parentheses indicate *Rattus norvegicus* protein accessions.

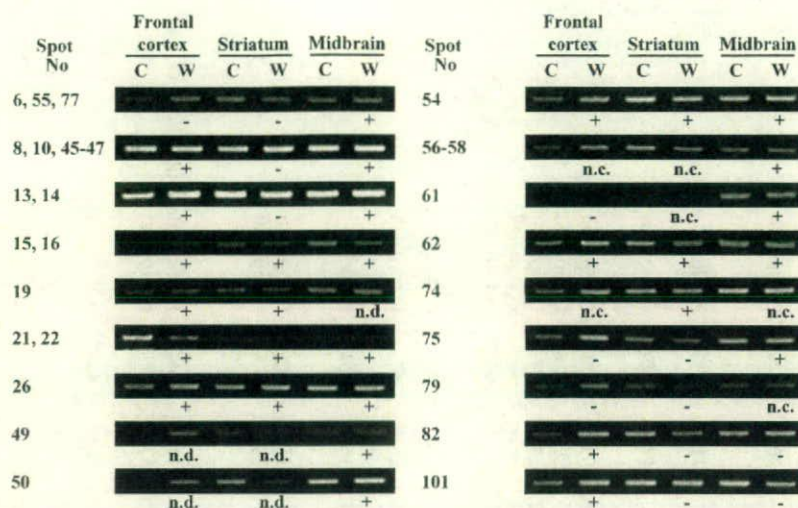
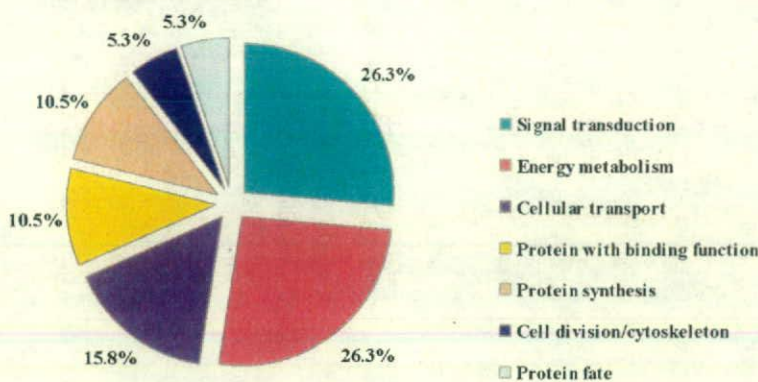


**Figure 5.** RT-PCR analysis of the genes encoding the differentially expressed proteins identified by 2-DGE. Protein spot numbers (the same as in Table 3) are given on the left-hand side of the gel image in parentheses. Marks and words given under gel images indicate expression changes of corresponding protein spots over controls on 2-D gel images of each brain regions. Plus (+) mean induced spots, minus (-) mean suppressed spots, and n.d., not detected; n.c., not changed; C, control; and W, Wig rat.

**A: Functional category**



**B: Subcellular localization**

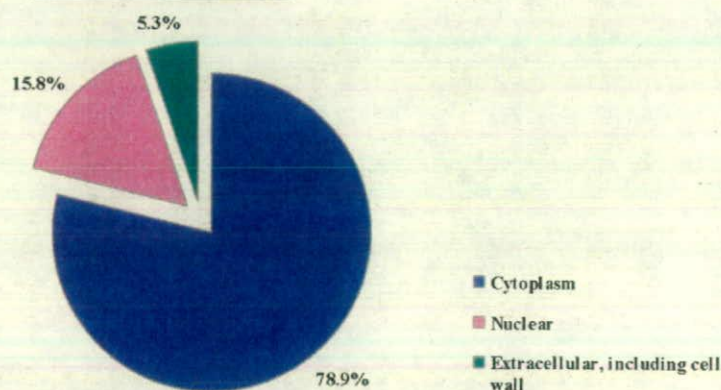


**Figure 6.** Functional categorization and subcellular localization of identified proteins. (A) The distribution of nonredundant proteins identified by MS analyses into functional categories determined using NCBI or Rat Genome Database; (B) the same (in above) protein distribution according to their subcellular localization determined using NCBI or Web tool PSORT II.

that the protein level of DRP2 was induced in anterior cingulate cortex of patients with schizophrenia (SCZ) and major depressive disorder (MDD).<sup>34,35</sup> CRMP2 and CRMP4 are also co-localized with F-actin of growth cone during discrete periods of neuronal development.<sup>36,37</sup> A recent report suggests that

overexpression of CRMP4 inhibit cell migration due to its specific regulatory role toward the actin cytoskeleton.<sup>36</sup> The CRMP4 and DRP2 proteins were found to be increased in the frontal cortex, speculating that induction of those proteins may cause the abnormality of axon guidance. Since we previously

observed a deficit in the development of DA neuron in Wig rats,<sup>8</sup> DA terminals should be investigated. However, multiple functional roles of CRMP4 and DRP2 are regulated via their phosphorylation by GSK3b,<sup>32,36</sup> and further research is necessary to reveal its role in the Wig rat brain.

Phosphatidylethanolamine binding protein (PEBP, spot 74), the precursor of the hippocampal cholinergic neurostimulating peptide (HCNP), is known to stimulate the enzymatic activity of choline acetyltransferase in cholinergic neurons following NMDA receptor activation.<sup>38</sup> This protein was increased in the striatum, suggesting the induction of acetylcholine synthesis. Cholinergic neurons also localize as interneuron in the striatum. Thus, this result speculates an impairment of the functional balance of afferent and efferent neurons in the striatum of Wig rat.

**3.3.2. Energy Metabolism.** A total of 5 proteins were classified into energy metabolism. One protein, fragile histidine triad (Fhit) protein (spot 26) having diadenosine 5',5''-P<sub>1</sub>P<sub>3</sub>-triphosphate (Ap3A) hydrolase activity in nucleotide metabolism was found to be increased in the frontal cortex. This protein is abundantly expressed in the brain and necessary for protecting cells from accumulation of DNA damage.<sup>39,40</sup> Brain glycogen phosphorylase (brain GPase, spot 50) is a brain-specific isoform of glycogen phosphorylase and is localized predominantly in astrocytes of the central nervous system (CNS).<sup>41</sup> GPase as the key enzyme in degradation of glycogen can provide energy for rapid neurotransmitter clearance by astrocytes.<sup>42</sup> A previous study has suggested that prolonged GPase activity might lead to impairment of energy state at the synapse due to deprivation of synaptic energy stores.<sup>43</sup> In our experiment, GPase protein was increased in the midbrain, which suggests the possibility of induction of glycogen degradation linked to supply glial energy. Another study also reported increased activity of GPase in the striatum of Huntington's disease (HD) model rat.<sup>44</sup> HD is characterized by the degeneration of striatal gamma-aminobutyric acid (GABA)-containing neurons. Although we do not observe alteration of GABAergic elements, the present results suggest its neurodegeneration in the midbrain of Wig rats. Phosphoglycerate mutase (D-phosphoglycerate 2,3-phosphomutase, PGM1; spot 62), a glycolytic enzyme that catalyzes the interconversion of 3-phosphoglycerate and 2-phosphoglycerate, was increased in the midbrain. Triosephosphate isomerase (Tpi) 1 protein (spot 101) is also a glycolytic enzyme that catalyzes the interconversion of dihydroxyacetone phosphate and glyceraldehyde 3-phosphate, and was found to be decreased in the midbrain. In a proteomics study of AD brains, the Tpi1 protein showed significant oxidative modification but not change in its activity.<sup>45</sup> It can be suggested that reduction of Tpi1 protein expression is linked to less enzymatic activity in the midbrain of Wig rat. Changes of these glycolytic enzymes suggest possibility of derangement of energy state in the midbrain of Wig rat.

Pyruvate dehydrogenase E1 alpha 1 (spot 82) is an E1 subunit member of pyruvate dehydrogenase complex.<sup>46</sup> This complex is a critical link between glycolysis and the tricarboxylic acid cycle catalyzing the oxidative decarboxylation of pyruvate in the formation of acetyl CoA in mitochondria.<sup>47</sup> We found pyruvate dehydrogenase E1 alpha 1 protein to be increased in the frontal cortex over control. It has also been shown that the E1 subunit is phosphorylated by GSK3b, which is linked to the reduction of the whole enzyme activity in  $\beta$ -amyloid peptide-treated hippocampal culture.<sup>48</sup> We speculate that the increase

in the protein could be due to its phosphorylation that however remains to be confirmed.

**3.3.3. Cellular Transport.** Three proteins were classified into cellular transport. D100 (also called as dynamin 1, spot 49), is a brain-specific isoform of dynamins and a microtubule-activated GTPase, which pinches off synaptic vesicles from the plasma membrane following fusion and exocytotic release of neurotransmitter.<sup>49,50</sup> Dynamin 1, which protein levels increase during neurite formation in vitro, is also involved in neuronal morphogenesis.<sup>50</sup> Previous reports have suggested that expression level changes of this protein might affect synaptic ability to successively release neurotransmitters as synaptic vesicles.<sup>49</sup> We show an increase of the dynamin 1 protein in the midbrain. This up-regulation may be involved in alteration of neurotransmitter release and neurite formation in neuron of the midbrain.

N-Ethylmaleimide sensitive fusion (NSF) protein attachment protein (SNAP)-beta (spot 75) is an isoform of SNAPS, and consists of three different isoforms, SNAP-alpha, -beta, and -gamma. In mammals, SNAP-alpha and -gamma are ubiquitously expressed, whereas SNAP-beta is the brain-specific isoform.<sup>51</sup> SNAPS recruit NSF to the membrane after being bound to specific membrane receptors termed SNAP receptors (SNAREs) and are related to intracellular membrane fusion and vesicular trafficking.<sup>52</sup> SNAP-beta interacts with the putative synaptic calcium sensor protein, synaptotagmin, and may be involved in calcium-regulated exocytosis.<sup>53</sup> In our experiment, SNAP-beta protein was increased in the midbrain, suggesting the induction of neurotransmitter release in the midbrain of Wig rat.

Syntaxin binding protein 1 (also called as Sec1 and Munc18, spot 79) that is specifically expressed in the brain was found to be decreased in the frontal cortex. Syntaxin binding protein 1 is involved in synaptic vesicle exocytosis and regulates the SNARE complex by binding to syntaxin 1A, which is a component of the target-SNARE (t-SNARE), due to inhibition of the interaction of syntaxin with SNAP25 and VAMP.<sup>54</sup> It can be speculated that the level of neurotransmitter release is reduced in the frontal cortex of Wig rat. These 3 proteins are involved in neurotransmitter release from synaptic vesicles. Moreover, among these 3 proteins, 2 proteins were found to be increased in the midbrain. Thus, our present results lead us to speculate that induction of these proteins may cause abnormality of synaptic vesicular transport in the midbrain.

**3.3.4. Protein with Binding Function.** Two proteins were classified into the binding function category. Calbindin 2 (also called as calretinin; spot 61) is a EF-hand calcium-binding protein, located in the midbrain, especially in the substantia nigra (SN) pars compacta, and may be involved in DA neurotransmission.<sup>55</sup> Interestingly, our previous report with macroarray analysis showed that the gene encoding this protein was increased in the midbrain of Wig rat during juvenile period.<sup>8</sup> In the present study, calbindin 2 protein was increased in the midbrain over control, supporting the previous study and showing a correlation between gene and protein expression. Solution structure of calcium-calmodulin N-terminal domain (spot 76) also showed an increase in the midbrain. Calmodulin is a ubiquitous Ca<sup>2+</sup>-binding protein with EF-hand, and in rat, 3 members, calmodulin 1, 2, and 3, have been identified. It has been suggested that calmodulin 1, expressed in neuronal tissues, acts as a mediator in the Ca<sup>2+</sup>-dependent modulation of KCNQ channels, which are involved in the control of cellular excitability.<sup>56</sup>

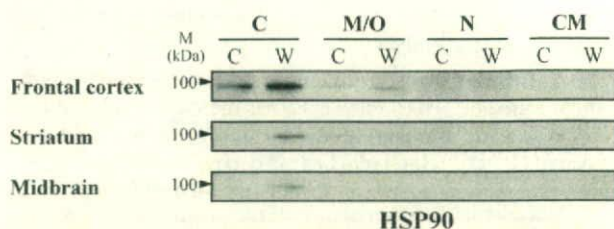


**Figure 7.** Western blot analysis of differentially expressed protein in the frontal cortex, striatum, and midbrain. Anti-HSP90 monoclonal antibody was used for detecting the cross-reacting proteins. C, control; W, Wig rat; C, cytosolic; M/O, membrane/organelle; N, nucleic, and CM, cytoskeletal matrix.

**3.3.5. Protein Synthesis.** Two proteins, a Tu translation elongation factor (EF-Tu, spot no 19) and an acidic ribosomal phosphoprotein P0 (spot no 54) were found to be increased in the frontal cortex and midbrain, respectively. The EF-Tu protein plays an important role in delivering aminoacyl-tRNA to the A-site on the ribosome of mitochondria. It has been recently suggested that mammalian EF-Tu might have chaperone activity in the quality control of misfolded newly synthesized polypeptides in mitochondria.<sup>57</sup> Interestingly, the acidic ribosomal phosphoprotein P0 constitutes a major part of the GTPase-associated center of eukaryotic ribosomes in translational machinery. Induction of these proteins suggests changes of protein state in the frontal cortex and midbrain. In the midbrain, increased EF-Tu protein may suggest presence of misfolded polypeptides.<sup>57</sup>

**3.3.6. Others.** CDCrel-1AI (spots 21 and 22) is classified into cell division/cytoskeleton category. The CDCrel-1 protein is also called septin 5, and is a member of the septin gene family that is predominantly expressed in the brain and localized mainly to presynaptic axon terminals of inhibitory neurons.<sup>58</sup> CDCrel-1 can negatively modulate neurotransmitter release due to inhibiting the formation of SNARE complex by directly binding to syntaxin-1.<sup>59</sup> It has been reported that the up-regulation of several synaptic scaffold proteins and several septins, including CDCrel-1, was observed in the cortex and striatum of the parkin knockout (KO) mice.<sup>60</sup> While, in parkin KO mice, it was reported no evidence for a loss of nigrostriatal dopaminergic neurons, we observed a loss of that in Wig rats.<sup>8,60</sup> In the present study, 2 protein spots identified as CDCrel-1AI were increased in the frontal cortex but not the striatum over control. This result may suggest that high expression of this protein might be a contributing factor causing an abnormality in neurotransmitter release in the frontal cortex.

Heat shock protein 90 alpha (HSP90a) protein (numbers 8, 10, 45, 46, and 47) was classified to protein fate. HSP90 is expressed constitutively in the brain from early development into adulthood and has two isoforms, alpha and beta, with similar functions.<sup>61</sup> HSP90 plays important roles as a chaperone, specifically involved in the folding or conformational regulation of central signal transduction molecules. Recently, it has been reported that HSP 90 is also involved in cell migration of the brain<sup>62</sup> and neurotransmitter release at presynaptic terminal in the hippocampus.<sup>63</sup> Interestingly, some studies have correlated the increased expression of HSP90 protein to aggregation of misfolded proteins in the human and rat brains of neurodegenerative disorders, such as Parkinson's disease and AD.<sup>64,65</sup> In our experiment, HSP90a was increased in the frontal cortex and midbrain. We performed Western analysis of this protein (Figure 7).

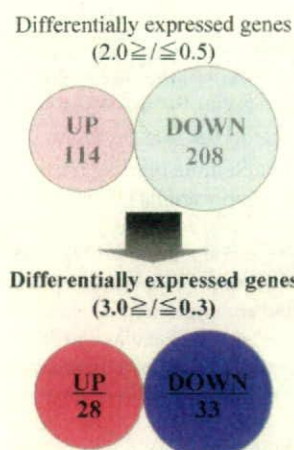


**Figure 8.** The number of differentially expressed genes. Schematic diagram shows the number of differentially expressed genes by microarray analysis in Wig rat brain. Light and dark pink circles indicate the up-regulated genes, above 2.0- and 3.0-fold, respectively. Light and dark blue circles indicate the down-regulated genes, respectively, at 0.5- and 0.3-fold. The number of altered genes was shown in each circle.

We confirmed the induction of HSP90 protein in cytosolic fraction of the frontal cortex and midbrain compared with control. We also detected the increment of this protein in cytosolic fraction of the striatum of Wig rat. This result is in line with the finding of increased HSP90 in the brains of patients with neurodegenerative disorders.

**3.4. Transcriptional Profiling of Differentially Expressed Genes in Wig Rat Brain.** To analyze the expression level of genes in brain regions of Wig rat, we checked the transcriptional levels of approximately 44 000 rat genes by using DNA microarray chip as mentioned in section 2.9. For the microarray experiment, the total RNA was pooled from the 3 brain regions (frontal cortex, striatum and midbrain) followed by cDNA synthesis, labeling and hybridization. After normalization, we summarized the genes whose transcriptional levels were altered more than 2-fold in Wig rat brain over the control. The results showed that 114 genes are up-regulated and 208 genes are down-regulated in the Wig rat brain (Figure 8). Using NCBI or RGD databases, these genes were categorized according to function (Supplementary Tables 2 and 3). Though a large number of genes were found to be induced/repressed, we selected genes with high fold-changes (more than 3-fold) over control for further discussion for clarity, and as these genes may be the most representative or related to the disorder in question, namely, ADHD. The results showed that 28 genes are highly up-regulated and 33 genes are highly down-regulated in the Wig rat brain. These genes were categorized according to function (Tables 5 and 6). Figure 9 shows gene distribution into functional categories. Finally, using independently derived cDNA from frontal cortex, striatum and midbrain total RNAs, we performed additional RT-PCR experiments to check and validate the individual patterns of mRNA expressions of some induced and suppressed genes. The results presented in Figure 10 further confirmed the reliability of the microarray

**Table 5.** List of Up-Regulated Genes (more than 3.0-fold) by Microarray Analysis<sup>a</sup>

gene	nucleotide accession (NCBI)	log	fold	description	reference
<i>Protein Fate</i>					
XM_232934	XR_008008	2.19	8.95	PREDICTED: <i>R. norvegicus</i> hypothetical LOC366706	
XM_236125	NM_001014089	1.78	5.92	<i>R. norvegicus</i> leucine rich repeat containing 35 (Lrrc35)	
A_43_P11766	NM_016998	1.37	3.92	<i>R. norvegicus</i> carboxypeptidase A1 (Cpa1)*	Normant et al., <sup>66</sup>
A_44_P516338	XM_001067936	1.13	3.09	PREDICTED: <i>R. norvegicus</i> similar to protein tyrosine phosphatase, receptor type, D (RGD1561090)*	Uetani et al., <sup>67</sup>
<i>Transcription</i>					
XM_343411	XR_009072	1.58	4.86	PREDICTED: <i>R. norvegicus</i> similar to c-myc promoter binding protein (RGD1562639)	
A_44_P399810	NM_002501	1.48	4.41	<i>Homo sapiens</i> nuclear factor 1/X (CCAAT-binding transcription factor) (NFIX)*	Gopalan et al., <sup>70</sup>
A_44_P350142	XM_001110382	1.44	4.21	PREDICTED: <i>Macaca mulatta</i> similar to T-box 4 (LOC712702)	
A_44_P491446	XM_001054651	1.31	3.72	PREDICTED: <i>R. norvegicus</i> DEAH (Asp-Glu-Ala-His) box polypeptide 15 (Dhx15)	
<i>Cellular Transport</i>					
XM_345372	XM_216315	2.28	9.75	PREDICTED: <i>R. norvegicus</i> six transmembrane epithelial antigen of the prostate 1 (Steap1)	
A_44_P479157	NM_031703	1.92	6.79	<i>R. norvegicus</i> aquaporin 3 (Aqp3)	
A_44_P181412	XM_001065495	1.52	4.56	PREDICTED: <i>R. norvegicus</i> similar to Coatomer gamma-2 subunit (Gamma-2 coat protein) (Gamma-2 COP) (RGD1566215)*	Blagitko et al., 1999 <sup>73</sup>
<i>Signal Transduction</i>					
XM_342830	XM_001071316	1.67	5.31	PREDICTED: <i>R. norvegicus</i> FERM and PDZ domain containing 1 (Frmpd1)	
WIG 2007-1		1.58	4.86		
A_44_P127638	NM_001025699	1.45	4.27	<i>R. norvegicus</i> macoilin (LOC313618)*	Kuvbachieva et al., <sup>75</sup>
<i>Cell Fate</i>					
A_44_P288849	XR_008769	1.23	3.41	PREDICTED: <i>R. norvegicus</i> NADH dehydrogenase (ubiquinone) 1 alpha subcomplex, 13 (Ndufa13)*	Lufei et al., <sup>88</sup>
A_44_P243874	NM_001081444	1.10	3.01	<i>R. norvegicus</i> similar to Expressed sequence BB220380 (RGD1560850)*	Voigt et al., <sup>89</sup>
<i>Protein with Binding Function</i>					
A_44_P182757	AF196258	1.73	5.65	<i>R. norvegicus</i> clone LRTVD8c4 T cell receptor V delta 8*	Hvas et al., <sup>95</sup>
A_44_P137517	NM_001009534	1.55	4.73	<i>R. norvegicus</i> similar to experimental autoimmune prostatitis antigen 2 (MGC72615)	
<i>Development</i>					
A_43_P12112	NM_021747	1.60	4.96	<i>R. norvegicus</i> acrosomal vesicle protein 1 (Acrv1)	
<i>Interaction with the Environment</i>					
A_44_P430517	BC081748	1.52	4.59	<i>R. norvegicus</i> sperm adhesion molecule	
<i>Energy and Metabolism</i>					
A_44_P399300	NM_001011945	1.69	5.42	<i>R. norvegicus</i> poly(rC) binding protein 3 (Pcbp3)*	Ko and Loh, <sup>80</sup>
<i>Unknown</i>					
A_44_P513918	AA924991	2.48	11.99	<i>R. norvegicus</i> cDNA clone UI-R-A1-eh-c-01-0-UI	
A_44_P409017	XM_001059479	1.45	4.25	PREDICTED: <i>R. norvegicus</i> RGD1565784 (RGD1565784)	
A_44_P340935	NM_001014102	1.41	4.10	<i>R. norvegicus</i> similar to 2810022L02Rik protein (RGD1309930)	
A_44_P422602	AI232943	1.29	3.62	EST229631 Normalized rat kidney, Bento Soares <i>Rattus</i> sp. cDNA clone RKICJ01	
A_44_P353367	BM384271	1.25	3.48	<i>R. norvegicus</i> cDNA clone UI-R-DZO-cks-m-09-0-UI	
A_43_P19341	XM_001070635	1.21	3.34	PREDICTED: <i>R. norvegicus</i> similar to GLI pathogenesis-related 2 (LOC684484)*	Murphy et al., <sup>108</sup>
A_44_P228145	BG381256	1.11	3.02	<i>R. norvegicus</i> cDNA clone UI-R-CT0-bui-a-09-0-UI	

<sup>a</sup> Asterisks and references indicate genes reported the expression in the brain and nervous systems.

experiment, and simultaneously revealed the expression profiles of these genes in the 3 individual brain regions.

**3.5. Overview of Changed Gene Expressions in the Brain.** Functional categorization of genes changed more 3-fold using NCBI and RGD gave 14 categories, namely, cell cycle and DNA processing, cell fate, cell division/cytoskeleton, cell rescue, cellular transport, development, energy, interaction with en-

vironment, metabolism, protein fate, protein synthesis, protein with binding function, signal transduction, and transcription (Figure 9, right panel). Out of the 28 up-regulated and 33 down-regulated genes, 7 and 9 genes, respectively, are unidentified or poorly characterized, indicating the incomplete (poor) annotation in the rat. Interestingly, 8 up-regulated genes were involved in protein fate and transcription, while the 10 down-

**Table 6.** List of Down-Regulated Genes (less than 0.3-fold) by Microarray Analysis<sup>a</sup>

gene	nucleotide accession (NCBI)	log	fold	description	reference
<i>Signal Transduction</i>					
WIG 2007-2		-2.52	0.08		
A_44_P251931	NM_001081216	-1.45	0.23	<i>M. musculus</i> pleckstrin homology domain interacting protein (Phip)*	Kato et al., <sup>76</sup>
A_44_P290488	NM_012872	-1.35	0.26	<i>R. norvegicus</i> phosducin (Pdc)*	Bauer et al., <sup>78</sup>
XM_344616	NM_001044251	-1.27	0.28	<i>R. norvegicus</i> similar to transmembrane receptor (MGC112790)	
A_44_P136059	NM_028407	-1.25	0.29	<i>M. musculus</i> granule cell antiserum positive 14 (Gcap14), transcript variant 2*	Kambouris et al., <sup>79</sup>
A_44_P346547	NM_001000282	-1.21	0.30	<i>R. norvegicus</i> olfactory receptor 440 (Olr440_predicted)	
<i>Energy and Metabolism</i>					
A_44_P437096	J02589	-1.52	0.22	<i>R. norvegicus</i> UDP glucuronosyltransferase precursor*	Martinasevic et al., <sup>82</sup>
A_44_P306204	X53501	-1.50	0.22	<b>Rat mRNA for tryptophan hydroxylase (EC 1.14.16.4)*</b>	<b>Tang et al.,<sup>107</sup></b>
A_44_P342320	XM_239062	-1.34	0.26	PREDICTED: <i>R. norvegicus</i> ectonucleoside triphosphate diphosphohydrolase 7 (Entpd7)*	Shi et al., <sup>85</sup>
A_44_P399015	XM_001062107	-1.28	0.28	PREDICTED: <i>R. norvegicus</i> ribose 5-phosphate isomerase A (Rpia)	
A_44_P150432	NM_001005888	-1.21	0.30	<b><i>R. norvegicus</i> galactosylceramidase (GalC)*</b>	<b>Suzuki and Suzuki,<sup>86</sup></b>
<i>Transcription</i>					
A_44_P574161	XR_007660	-1.29	0.28	PREDICTED: <i>R. norvegicus</i> similar to hypothetical protein (RGD1562123)	
A_44_P361189	XR_008141	-1.26	0.28	PREDICTED: <i>R. norvegicus</i> similar to transcription factor ONECUT2 (RGD1564677)	
A_44_P177398	NM_199373	-1.24	0.29	<i>R. norvegicus</i> tryptophan rich basic protein (Wrb)*	Egeo et al., <sup>71</sup>
A_44_P367880	XM_218245	-1.22	0.29	PREDICTED: <i>R. norvegicus</i> oocyte specific homeobox 2 (Obox2)	
<i>Cellular Transport</i>					
A_44_P394305	NM_001009713	-1.44	0.24	<b><i>R. norvegicus</i> solute carrier family 17 (anion/sugar transporter), member 5 (Slc17a5)*</b>	<b>Verheijen et al.,<sup>74</sup></b>
A_44_P468972	XM_234725	-1.30	0.27	PREDICTED: <i>R. norvegicus</i> similar to ATP-binding cassette, subfamily B, member 5 (RGD1566342)	
<i>Protein with Binding Function</i>					
A_44_P338632	NM_080770	-1.62	0.20	<i>R. norvegicus</i> secretoglobulin, family 2A, member 1 (Scgb2a1)	
A_44_P244607	NM_001024205	-1.23	0.29	<b><i>M. musculus</i> nuclear fragile X mental retardation protein interacting protein 2 (Nufip2)*</b>	<b>Bardoni et al.,<sup>97</sup></b>
<i>Cell Cycle and DNA Processing</i>					
A_44_P481541	NM_053394	-1.25	0.29	<i>R. norvegicus</i> Kruppel-like factor 5 (Klf5)	
<i>Cell Division/Cytoskeleton</i>					
XM_345389	XM_001076779	-1.48	0.23	PREDICTED: <i>R. norvegicus</i> similar to copine VIII isoform 1 (LOC499828)*	Maitra et al., <sup>102</sup>
<i>Cell Fate</i>					
A_44_P294571	EF125690	-1.72	0.18	<b><i>R. norvegicus</i> brain-derived neurotrophic factor precursor transcript variant IXA (Bdnf)*</b>	<b>Mogi et al.,<sup>92</sup></b>
<i>Cell Rescue, Defense and Virulence</i>					
A_44_P271423	NM_173045	-1.38	0.25	<i>R. norvegicus</i> zinc finger CCCH type, antiviral 1 (Zc3hav1)*	Yue et al., <sup>103</sup>
<i>Protein Fate</i>					
A_44_P493505	NM_153573	-1.55	0.21	<i>M. musculus</i> FK506 binding protein 14 (Fkbp14)	
<i>Protein Synthesis</i>					
XM_346027	BC058468	-1.38	0.25	<i>R. norvegicus</i> ribosomal protein L10A*	Xia et al., <sup>105</sup>
<i>Unknown</i>					
A_44_P210002	XR_008649	-1.67	0.19	PREDICTED: <i>R. norvegicus</i> hypothetical protein LOC684268	
A_44_P314146	XM_001064598	-1.57	0.21	PREDICTED: <i>R. norvegicus</i> similar to spermatogenesis associated glutamate (E)-rich protein 4d (LOC685632)	
A_44_P296380	XM_001058484	-1.57	0.21	PREDICTED: <i>R. norvegicus</i> similar to hypothetical protein MGC38960 (RGD1310552)	
A_44_P255084	AY383691	-1.36	0.26	<i>R. norvegicus</i> LRRGT00036	
A_44_P251312	AA818416	-1.30	0.27	<i>R. norvegicus</i> cDNA clone UI-R-A0-au-f-04-0-UI	
XM_341787	AY310139	-1.29	0.28	<i>R. norvegicus</i> Ac1071	
A_44_P260765	AA924536	-1.27	0.28	<i>R. norvegicus</i> cDNA clone UI-R-A1-dz-e-06-0-UI	
A_44_P252250	XM_001081031	-1.26	0.28	PREDICTED: <i>R. norvegicus</i> similar to RIKEN cDNA 1190005P17 (RGD1308261)	

<sup>a</sup> Bold letters indicate genes reported to be involved in neurological disorders. Asterisks and references indicate genes reported the expression in the brain and nervous systems.

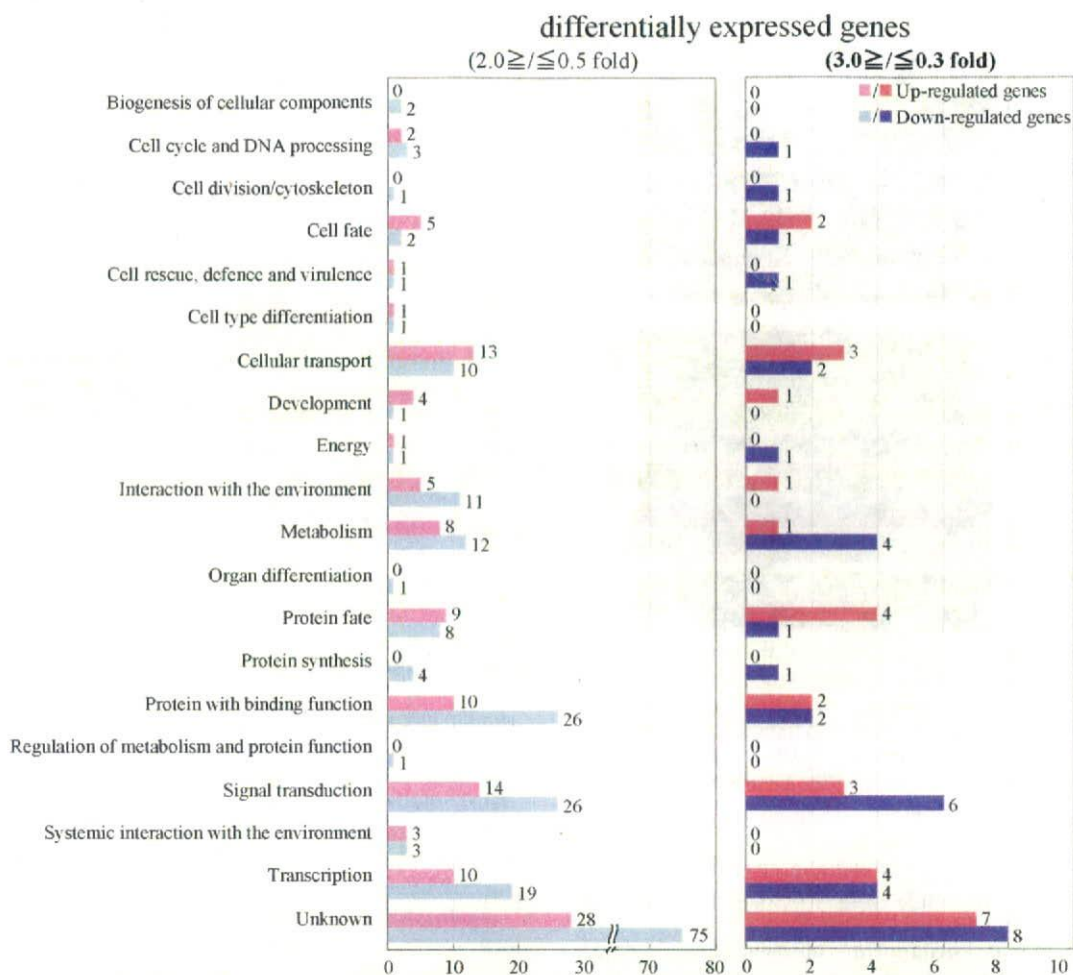


**Figure 9.** Functional categorization of differentially expressed genes. The left panel shows the distribution of up- and down-regulated genes ( $\geq 2.0$ -fold for increment or  $\leq 0.5$ -fold for decrement) in Wig rat into functional categories determined using NCBI or Rat Genome Database. The right panel shows the distribution of up- and down-regulated genes ( $\geq 3.0$ -fold for increment or  $\leq 0.3$ -fold for decrement) in Wig rat into functional categories. Light and dark pink bars indicate the up-regulated genes. Light and dark blue bars indicate the down-regulated genes.

regulated genes were involved in metabolism and signal transduction.

**3.5.1. Protein Fate.** Four up-regulated and 1 down-regulated genes were classified into protein fate. NM\_001014089 (leucine rich repeat containing 35), with a conserved domain which is closely related to the ubiquitin-like domain of a family of deubiquitinases, has putative role in protein modification process. NM\_016998 (carboxypeptidase A1) is an exopeptidase that plays a role in protein catabolism, and has low-abundance expression of the mRNA in the CNS.<sup>66</sup> XM\_001067936 (similar to protein tyrosine phosphatase, receptor type, D) belongs to a leukocyte common antigen-related subfamily of receptor protein tyrosine phosphatases and is abundantly expressed in the CNS during neural development. Protein tyrosine phosphatase receptor type D contributes to appropriate motor-neuron axon targeting during mammalian axonogenesis.<sup>67</sup> NM\_153573 (FK506 binding protein 14, Fkbp14), also known as Fkbp22, is a member of numerous FKBP family with different characteristics. Fkbp22, with peptidyl-prolyl *cis/trans* isomerase (PPIase) activity, was identified as a novel chaperone in the endoplasmic reticulum of *Neurospora crassa*.<sup>68</sup> It suggested that Fkbp22 has a role in ER network as a member of chaperone/folding complexes.

**3.5.2. Transcription.** Four up-regulated and 4 down-regulated genes were classified into transcription. NM\_002501 (nuclear factor I/X, CCAAT-binding transcription factor, NFIX) is a member of nuclear factor (NF) 1 family whose proteins are associated with transcriptional regulation of cellular and viral genes.<sup>69</sup> A recent report has suggested that NF1, including NF1X, is indispensable for regulation of the specific gene expression in astrocytes.<sup>70</sup> NM\_199373 (tryptophan rich basic protein, Wrb) is localized in nucleus but its function is not well-known. However, it has been reported that the *Wrb* gene is abundantly expressed in several tissues including the fetal and adult brain and may be involved in transcriptional processes.<sup>71</sup>

**3.5.3. Cellular Transport.** Three up-regulated and 2 down-regulated genes were classified into cellular transport. NM\_031703 (aquaporin 3, aqp3), a member of aquaporin (AQP) family which plays a role in fluid transport, is expressed in several tissues including kidney and eye but not brain, and is permeable to glycerol.<sup>72</sup> XM\_001065495 (similar to coatmer gamma-2 subunit), also known as Gamma-2 coat protein and Gamma-2 COP, is expressed in fetal and adult brain, and has a role for cellular vesicle trafficking.<sup>73</sup> NM\_001009713 [solute carrier family 17 (anion/sugar transporter), member 5], encoding sialin, functions as a lysosomal sialic acid transporter.

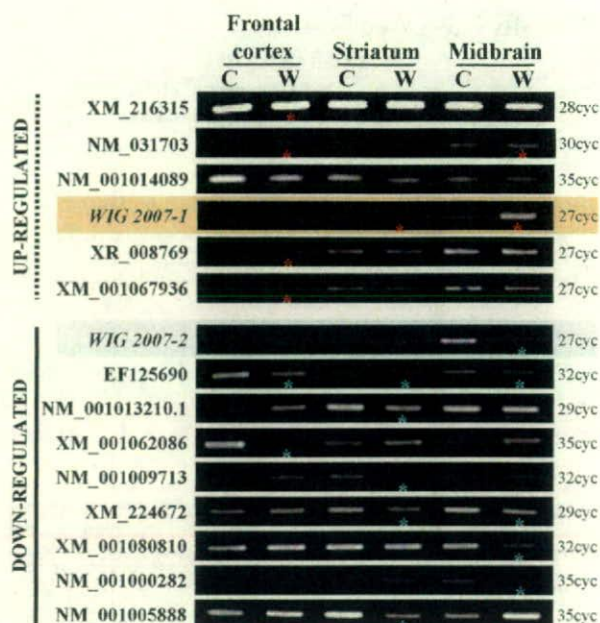


**Figure 10.** Validatory RT-PCR analysis of the differentially expressed genes. Gene names are given on the left-hand side of the gel images, and are subdivided into up-regulated and down-regulated genes. The PCR cycles are marked on the right-hand side. Asterisks indicate the clearly up- and down-regulated genes (in right panel, Figure 9) among the frontal cortex, striatum, and midbrain. C: control; W, Wistar rat.

Previous study has shown that mutations on sialin caused Salla disease and sialic acid storage disorder, which are autosomal recessive neurodegenerative diseases.<sup>74</sup>

**3.5.4. Signal Transduction.** Three up-regulated and 6 down-regulated genes were classified into signal transduction. NM\_001025699 (macoilin), also known as transmembrane 57 and Tmem57, was identified as a brain-specific and developmentally regulated gene and is predominantly expressed in differentiating neurons.<sup>75</sup> It has been suggested that macoilin protein has a role in axonal traffic or signaling.<sup>75</sup> NM\_001081216 (pleckstrin homology domain interacting protein), also known as neuronal differentiation related protein, is predominantly expressed in developing and regenerating neurons.<sup>76</sup> This protein stably associates with insulin receptor substrate -1 (IRS-1) in vivo and may be involved in the development of sensory neurons.<sup>76,77</sup> NM\_012872 (phosducin) is a major protein constituent of retinal photoreceptor cells and pinealocytes and binds to the transducin  $\beta\gamma$  subunits. Phosducin, expressed at lower level in the brain, is known to be a protein kinase-regulated G-protein regulator.<sup>78</sup> NM\_028407 (granule cell antiserum positive 14 transcript variant 2) is one of the expressed genes in cerebellar granule cells.<sup>79</sup> However, the functional role of these genes remains to be determined. We would briefly like to mention about two genes in this category, namely, *WIG 2007-1* and *-2* (see Figure 10, and Tables 5 and 6) which were highly induced and repressed, respectively. These genes/gene products may serve as potentially promising and important markers for ADHD, and we are in the process of functionally analyzing and patenting them; therefore, we cannot discuss more on these 2 genes.

**3.5.5. Energy and Metabolism.** One up-regulated and 5 down-regulated genes were classified into energy and metabolism. NM\_001011945 (poly(rC) binding protein 3), an isoform

of poly(rC) binding proteins (PCBPs), is involved in mRNA metabolism. PCBPs bind to single-stranded DNA and participate in regulation of neuronal mu-opioid receptor expression, which plays a key role in mediating the major clinic effects of analgesics, such as morphine.<sup>80</sup> J02589 (UDP glucuronosyltransferase (UGT) precursor) produces the UGT 2 family polypeptide B (UGT2B2), which belongs to UGT superfamily, and is constitutively expressed in rat liver.<sup>81</sup> The UGT superfamily members catalyze the conversion of endobiotics and xenobiotics to glucuronides. Previously, the UGT1A6 but not UGT2B2 immunoactivity was detected in the rat brain.<sup>82</sup> X53501 (tryptophan hydroxylase, TPH) has two isoforms, TPH1 and 2, and is abundantly expressed in the midbrain. TPH, the rate limiting enzyme in serotonin biosynthesis, is one of the most important regulating factors in the serotonergic system. Interestingly, a previous report has suggested the association of TPH gene with ADHD in Chinese Han Population.<sup>83</sup> Contrastingly, other report suggests that the TPH2 gene polymorphisms have no association with ADHD in Irish patients.<sup>84</sup> Our present result showed the down-regulation of TPH1 but not TPH2. XM\_239062 (ectonucleoside triphosphate diphosphohydrolase 7), also known as *Lalp1* in mouse and human, is a member of endoapyrase family and expressed in most tissues including brain.<sup>85</sup> It has been suggested that endoapyrases may be critical for regulating the level of activated sugar during protein glycosylation.<sup>85</sup> NM\_001005888 (galactosylceramidase), also known as *Galc*, is a lysosomal enzyme that catalyzes the digestion of its major substrate galactocerebroside in myelinating oligodendrocytes and Schwann cells.<sup>86</sup> Genetic deficiency of *Galc* activity causes a lysosomal storage disease known as Globoid cell leukodystrophy with severe neurological symptoms such as intension tremor.<sup>87</sup>

**3.5.6. Others.** Two up-regulated and 1 down-regulated genes were classified into cell fate. XR\_008769 (NADH dehydrogenase (ubiquinone) 1 alpha subcomplex, 13), a gene associated with retinoid-interferon (IFN)-induced mortality (GRIM) 19, is highly expressed in the brain. GRIM19 protein is primarily localized in the mitochondria and promotes cell death induced by IFN and retinoic acid.<sup>88</sup> NM\_001081444 (similar to Expressed sequence BB220380) encodes for a p87 phosphoinositide 3-kinase (PI3K) gamma adapter protein, a regulatory subunit of PI3K gamma which is activated by G protein-coupled receptors (GPCRs).<sup>89</sup> It has been shown that expression change of the PI3K gamma protein contributes to supraspinal antinociception in mouse brain.<sup>90</sup> EF125690 [brain-derived neurotrophic factor (BDNF) precursor transcript variant IXA] is a member of the neurotrophin family of secreted growth factors vital for support of neurons within the CNS and plays role in regulating neuronal survival, differentiation, and synaptic plasticity. The depletion of BDNF caused derangement of dopaminergic neurons in the midbrain of knockout mouse.<sup>91</sup> Several studies have reported that BDNF reduction is related to neurological diseases, such as PD and HD.<sup>92,93</sup>

Two up-regulated and 2 down-regulated genes were classified into protein with binding function. AF196258 (T cell receptor V delta 8) is a member of delta T cell receptors and has a role for binding with interacting proteins.<sup>94</sup> Some genes encoding delta T cell receptors are involved in pathogenesis of multiple sclerosis.<sup>95</sup> NM\_080770 (secretoglobin, family 2A, member 1, scgb2a1), also known as prostatic steroid binding protein 1, is expressed in the prostate and is a small protein of unknown function in vivo.<sup>96</sup> Its promoter region contains an androgen responsive element. NM\_001024205 (nuclear fragile



X mental retardation protein interacting protein 2), also known as Nufip2 and 82-FIP, is expressed in neurons of the CNS and is associated with polyribosomes which is a component of fragile X mental retardation protein-containing mRNA-protein.<sup>97</sup>

NM\_021747 (acrosomal vesicle protein 1, also known as sperm protein 10) is a testis-specific differentiation antigen human homologue,<sup>98</sup> and is involved in development. BC081748 (sperm adhesion molecule, also known as SPAM1, 2B1 or PH-20) is a plasma membrane-bound glycoprotein with hyaluronidase activity and involved in cross-talk between the tubule epithelium and lumicrine factors in the epididymis.<sup>99</sup> NM\_053394 (Kruppel-like factor 5), also known as basic transcription element binding protein (BTEB) 2, is a member of Kruppel-like factors (KLFs) which belong to a class of zinc finger-containing transcription factors.<sup>100</sup> Previous report has shown that down-regulation of KLF5 expression by inhibiting the promoter activity results in a reduction of cell proliferation rate in the intestinal epithelial cell line.<sup>101</sup> Our present results show suppression in the expression level of the KLF5 mRNA. In agreement with a previous report, the reduction of KLF5 may indicate a possibility of latency of cell proliferation in the brain of Wig rats. XM\_001076779 (similar to copine VIII isoform 1), recently identified in human, is a new member of the copine family that may play a critical role in development and mitogenesis and has two isoforms.<sup>102</sup> Copine 8 is highly expressed in the prostate, heart, and brain, and is a calcium-dependent, phospholipid-binding protein.<sup>102</sup> However, the functional role of copine 8 in the brain is not well-clarified. NM\_173045 (zinc finger CCCH type, antiviral 1), also known as Zap, is a host antiviral factor, is reported the expression in various tissues, including human brain.<sup>103</sup> Zap specifically inhibits the replication of virus by preventing the accumulation of viral RNA in the cytoplasm.<sup>104</sup> BC058468 (ribosomal protein L10A) is a subunit of 60S ribosomal proteins and may be involved in ribosome resembling, protein synthesis, oxidative stress response, and immunosuppressive events.<sup>105</sup>

#### 4. Conclusions

We believe that along with genomics (and at a later stage the metabolite components) proteomic analysis of brain/brains regions may help to understand the complexity, to investigate disorders of the CNS, and to search for corresponding early markers. Our gel-based proteomics study is a first such investigation on surveying the Wig rat brain protein for identifying differentially expressed proteins in the frontal cortex, striatum, and midbrain. Using 2-DGE in conjunction with MS resulted in the identification of 19 nonredundant proteins. Among these, 5 proteins (dynamitin 1, SNAP-beta, syntaxin binding protein 1, calbindin 2, and CDCrel-1AI) are involved in neurotransmitter release, of which 3 proteins were up-regulated in the midbrain. It can be suggested that induction of these proteins may cause abnormality of synaptic vesicular transport in the midbrain. Moreover, expression levels of various proteins (14-3-3 proteins, DRP-2, PEBP, brain GPase, PGM1, Tpi1, dynamitin 1, CDCrel-1AI, HSP90a) have been suggested to be changed in neurodegenerative and psychiatric disorders. The activities of some of differentially expressed proteins have been reported to be regulated by phosphorylation.<sup>32,36,48,106</sup> Thus, it will be necessary to investigate functional activity of the proteins in Wig rat brain. The complete nature of biological samples cannot be accurately clarified by 2-DGE alone.

Moreover, 2-DGE will require future studies using complementary approaches to solve its inherent problems (for basic, membrane, small, high, and low pI proteins). These approaches, actively considered in our future studies, are 1-DGE in conjunction with protein identification by MS, and LC with MS (MudPIT, multidimensional protein identification technology) following trypsin digestion of samples. On the other hand, a parallel study of transcript profiling in Wig rat brains revealed 28 up-regulated genes and 33 down-regulated genes. Some genes had already been independently identified by studies of neurological disorders, such as AD and fragile X syndrome. Interestingly, out of the down-regulated genes, 1 gene encoding tryptophan hydroxylase was reported to possess a mutation in the Chinese patients with ADHD.<sup>83</sup> Finally, in both proteomics and transcriptomics levels, it is necessary to investigate the consequence of differential expression changes in Wig rat brain, ultimately leading to uncover the pathogenesis of ADHD.

**Acknowledgment.** We are extremely grateful for the expert technical support on use of the Agilent scanner by Drs. Kouji Satoh and Shoshi Kikuchi of the Plant Genome Research Unit, National Institute of Agrobiological Sciences, Tsukuba, Japan.

**Supporting Information Available:** Tables of peptide information of the MS-identified protein spots, and lists of up-regulated genes (more than 2.0-fold) and down-regulated genes (less than 0.5-fold) by microarray analysis. This material is available free of charge via the Internet at <http://pubs.acs.org>.

#### References

- (1) Russell, V. A. *Neurosci. Biobehav. Rev.* **2003**, *27*, 671–682.
- (2) Viggiano, D.; Vallone, D.; Ruocco, L. A.; Sadile, A. G. *Neurosci. Biobehav. Rev.* **2003**, *27*, 683–689.
- (3) Russell, V. A. *J. Neurosci. Methods* **2007**, *161*, 185–198.
- (4) Kamimura, E.; Ueno, Y.; Tanaka, S.; Sawa, H.; Yoshioka, M.; Ueno, K. I.; Inoue, T.; Li, X.; Koyama, T.; Ishikawa, R.; Nagashima, K. *Comp. Med.* **2001**, *51*, 245–251.
- (5) Davids, E.; Zhang, K.; Kula, N. S.; Tarazi, F. I.; Baldessarini, R. J. *J. Pharmacol. Exp. Ther.* **2002**, *301*, 1097–1102.
- (6) Zhang, K.; Tarazi, F. I.; Baldessarini, R. J. *Neuropsychopharmacology* **2001**, *25*, 624–632.
- (7) Masuo, Y.; Ishido, M.; Morita, M.; Oka, S.; Niki, E. *J. Neurochem.* **2004**, *91*, 9–19.
- (8) Masuo, Y.; Ishido, M.; Morita, M.; Sawa, H.; Nagashima, K.; Niki, E. *Eur. J. Neurosci.* **2007**, *25*, 3659–3666.
- (9) Sonuga-Barke, E. J. *Neurosci. Biobehav. Rev.* **2003**, *27*, 593–604.
- (10) Fountoulakis, M.; Kossida, S. *Electrophoresis* **2006**, *27*, 1556–1573.
- (11) Yang, L.; Sun, Z. S.; Zhu, Y. P. *J. Proteome Res.* **2007**, *6*, 2239–2247.
- (12) Almeras, L.; Eyles, D.; Benech, P.; Laffite, D.; Villard, C.; Patatian, A.; Boucraut, J.; Mackay-Sim, A.; McGrath, J.; Feron, F. *Proteomics* **2007**, *7*, 769–780.
- (13) Zhang, L.; Jie, C.; Obie, C.; Abidi, F.; Schwartz, C. E.; Stevenson, R. E.; Valle, D.; Wang, T. *Genome Res.* **2007**, *17*, 641–648.
- (14) DeRisi, J. L.; Iyer, V. R.; Brown, P. O. *Science* **1997**, *278*, 680–686.
- (15) Arion, D.; Unger, T.; Lewis, D. A.; Mirnics, K. *Eur. J. Neurosci.* **2007**, *25*, 1843–1854.
- (16) Hirano, M.; Rakwal, R.; Shibato, J.; Agrawal, G. K.; Jwa, N. S.; Iwahashi, H.; Masuo, Y. *Mol. Cells* **2006**, *22*, 119–125.
- (17) Gygi, S. P.; Rochon, Y.; Franza, B. R.; Aebersold, R. *Mol. Cell. Biol.* **1999**, *19*, 1720–1730.
- (18) Masuo, Y.; Ishido, M.; Morita, M.; Oka, S. *Neural Plast.* **2004**, *11*, 59–76.
- (19) Glowinski, J.; Iversen, L. L. *J. Neurochem.* **1966**, *13*, 655–669.
- (20) Hirano, M.; Rakwal, R.; Kouyama, N.; Katayama, Y.; Hayashi, M.; Shibato, J.; Ogawa, Y.; Yoshida, Y.; Iwahashi, H.; Masuo, Y. *J. Proteome Res.* **2007**, *6*, 2656–2668.
- (21) Perkins, D. N.; Pappin, D. J.; Creasy, D. M.; Cottrell, J. S. *Electrophoresis* **1999**, *20*, 3551–3567.
- (22) Shevchenko, A.; Wilm, M.; Vorm, O.; Mann, M. *Anal. Chem.* **1996**, *68*, 850–858.

- (23) Jung, Y. H.; Rakwal, R.; Agrawal, G. K.; Shibato, J.; Kim, J. A.; Lee, M. O.; Choi, P. K.; Jung, S. H.; Kim, S. H.; Koh, H. J.; Yonekura, M.; Iwahashi, H.; Jwa, N. S. *J. Proteome Res.* **2006**, *5*, 2586–2598.
- (24) Rosenzweig, B. A.; Pine, P. S.; Doman, O. E.; Morris, S. M.; Chen, J. J.; Sistare, F. D. *Environ. Health Perspect.* **2004**, *112*, 480–487.
- (25) Altman, N. *Appl. Bioinf.* **2005**, *4*, 33–44.
- (26) Martin-Magniette, M. L.; Aubert, J.; Cabannes, E.; Daudin, J. J. *Bioinformatics* **2005**, *21*, 1995–2000.
- (27) Cho, K.; Agrawal, G. K.; Shibato, J.; Jung, Y. H.; Kim, Y. K.; Nahm, B. H.; Jwa, N. S.; Tamogami, S.; Han, O.; Kohda, K.; Iwahashi, H.; Rakwal, R. *J. Proteome Res.* **2007**, *6*, 3581–3603.
- (28) Umahara, T.; Uchihara, T.; Tsuchiya, K.; Nakamura, A.; Iwamoto, T.; Ikeda, K.; Takasaki, M. *Acta Neuropathol. (Berlin)* **2004**, *108*, 279–286.
- (29) Fountoulakis, M.; Cairns, N.; Lubec, G. *J. Neural Transm. Suppl.* **1999**, *57*, 323–335.
- (30) Satoh, J.; Yamamura, T.; Arima, K. *Am. J. Pathol.* **2004**, *165*, 577–592.
- (31) Layfield, R.; Fergusson, J.; Aitken, A.; Lowe, J.; Landon, M.; Mayer, R. *J. Neurosci. Lett.* **1996**, *209*, 57–60.
- (32) Yoshimura, T.; Kawano, Y.; Arimura, N.; Kawabata, S.; Kikuchi, A.; Kaibuchi, K. *Cell* **2005**, *120*, 137–149.
- (33) Fukata, Y.; Itoh, T. J.; Kimura, T.; Menager, C.; Nishimura, T.; Shiromizu, T.; Watanabe, H.; Inagaki, N.; Iwamatsu, A.; Hotani, H.; Kaibuchi, K. *Nat. Cell Biol.* **2002**, *4*, 583–591.
- (34) Paulson, L.; Martin, P.; Nilsson, C. L.; Ljung, E.; Westman-Brinkmalm, A.; Blennow, K.; Davidsson, P. *Proteomics* **2004**, *4*, 819–825.
- (35) Beasley, C. L.; Pennington, K.; Behan, A.; Wait, R.; Dunn, M. J.; Cotter, D. *Proteomics* **2006**, *6*, 3414–3425.
- (36) Rosslenbroich, V.; Dai, L.; Baader, S. L.; Noegel, A. A.; Gieselmann, V.; Kappler, J. *Exp. Cell Res.* **2005**, *310*, 434–444.
- (37) Wang, L. H.; Strittmatter, S. M. *J. Neurosci.* **1996**, *16*, 6197–6207.
- (38) Iwase, T.; Ojika, K.; Matsukawa, N.; Nishino, H.; Yamamoto, T.; Okada, H.; Fujimori, O.; Ueda, R. *Neuroscience* **2001**, *102*, 341–352.
- (39) Ishii, H.; Wang, Y.; Huebner, K. *Cell Cycle* **2007**, *6*, 1044–1048.
- (40) Golebiowski, F.; Kowara, R.; Pawelczyk, T. *Mol. Cell. Biochem.* **2001**, *226*, 49–55.
- (41) Ignacio, P. C.; Baldwin, B. A.; Vijayan, V. K.; Tait, R. C.; Gorin, F. A. *Brain Res.* **1990**, *529*, 42–49.
- (42) Shulman, R. G.; Hyder, F.; Rothman, D. L. *Proc. Natl. Acad. Sci. U.S.A.* **2001**, *98*, 6417–6422.
- (43) Poblete, J. C.; Azmitia, E. C. *Brain Res.* **1995**, *680*, 9–15.
- (44) Levivier, M.; Donaldson, D. *Neurol. Res.* **2000**, *22*, 425–429.
- (45) Sultana, R.; Boyd-Kimball, D.; Poon, H. F.; Cai, J.; Pierce, W. M.; Klein, J. B.; Merchant, M.; Markesbery, W. R.; Butterfield, D. A. *Neurobiol. Aging* **2006**, *27*, 1564–1576.
- (46) Martin, E.; Rosenthal, R. E.; Fiskum, G. *J. Neurosci. Res.* **2005**, *79*, 240–247.
- (47) Reed, L. J. *J. Biol. Chem.* **2001**, *276*, 38329–38336.
- (48) Hoshi, M.; Takashima, A.; Noguchi, K.; Murayama, M.; Sato, M.; Kondo, S.; Saitoh, Y.; Ishiguro, K.; Hoshino, T.; Imahori, K. *Proc. Natl. Acad. Sci. U.S.A.* **1996**, *93*, 2719–2723.
- (49) Kelly, B. L.; Ferreira, A. J. *J. Biol. Chem.* **2006**, *281*, 28079–28089.
- (50) Torre, E.; McNiven, M. A.; Urrutia, R. *J. Biol. Chem.* **1994**, *269*, 32411–32417.
- (51) Puschel, A. W.; O'Connor, V.; Betz, H. *FEBS Lett.* **1994**, *347*, 55–58.
- (52) Clary, D. O.; Griff, I. C.; Rothman, J. E. *Cell* **1990**, *61*, 709–721.
- (53) Stenbeck, G. *Int. J. Biochem. Cell Biol.* **1998**, *30*, 573–577.
- (54) Mitchell, S. J.; Ryan, T. A. *Neuropharmacology* **2005**, *48*, 372–380.
- (55) Gonzalez-Hernandez, T.; Rodriguez, M. *J. Comp. Neurol.* **2000**, *421*, 107–135.
- (56) Yus-Najera, E.; Santana-Castro, I.; Villarroel, A. *J. Biol. Chem.* **2002**, *277*, 28545–28553.
- (57) Suzuki, H.; Ueda, T.; Taguchi, H.; Takeuchi, N. *J. Biol. Chem.* **2007**, *282*, 4076–4084.
- (58) Kinoshita, A.; Noda, M.; Kinoshita, M. *J. Comp. Neurol.* **2000**, *428*, 223–239.
- (59) Beites, C. L.; Xie, H.; Bowser, R.; Trimble, W. S. *Nat. Neurosci.* **1999**, *2*, 434–439.
- (60) Periquet, M.; Corti, O.; Jacquier, S.; Brice, A. *J. Neurochem.* **2005**, *95*, 1259–1276.
- (61) D'Souza, S. M.; Brown, I. R. *Cell Stress Chaperones* **1998**, *3*, 188–199.
- (62) Sidera, K.; Samiotaki, M.; Yfanti, E.; Panayotou, G.; Patsavoudi, E. *J. Biol. Chem.* **2004**, *279*, 45379–45388.
- (63) Gerges, N. Z.; Tran, I. C.; Backos, D. S.; Harrell, J. M.; Chinkers, M.; Pratt, W. B.; Esteban, J. A. *J. Neurosci.* **2004**, *24*, 4758–4766.
- (64) Takata, K.; Kitamura, Y.; Tsuchiya, D.; Kawasaki, T.; Taniguchi, T.; Shimohama, S. *Neurosci. Lett.* **2003**, *344*, 87–90.
- (65) Uryu, K.; Richter-Landsberg, C.; Welch, W.; Sun, E.; Goldbaum, O.; Norris, E. H.; Pham, C. T.; Yazawa, I.; Hilburger, K.; Micsenyi, M.; Giasson, B. I.; Bonini, N. M.; Lee, V. M.; Trojanowski, J. Q. *Am. J. Pathol.* **2006**, *168*, 947–961.
- (66) Normant, E.; Gros, C.; Schwartz, J. C. *J. Biol. Chem.* **1995**, *270*, 20543–20549.
- (67) Uetani, N.; Chagnon, M. J.; Kennedy, T. E.; Iwakura, Y.; Tremblay, M. L. *J. Neurosci.* **2006**, *26*, 5872–5880.
- (68) Tremmel, D.; Duarte, M.; Videira, A.; Tropschug, M. *FEBS Lett.* **2007**, *581*, 2036–2040.
- (69) Ravichandran, V.; Sabath, B. F.; Jensen, P. N.; Houff, S. A.; Major, E. O. *J. Virol.* **2006**, *80*, 10506–10513.
- (70) Gopalan, S. M.; Wilczynska, K. M.; Konik, B. S.; Bryan, L.; Kordula, T. *J. Biol. Chem.* **2006**, *281*, 13126–13133.
- (71) Egeo, A.; Mazzocco, M.; Sotgia, F.; Arrigo, P.; Oliva, R.; Bergonon, S.; Nizetic, D.; Rasore-Quartino, A.; Scartezzini, P. *Hum. Genet.* **1998**, *102*, 289–293.
- (72) Ishibashi, K.; Sasaki, S.; Fushimi, K.; Uchida, S.; Kuwahara, M.; Saito, H.; Furukawa, T.; Nakajima, K.; Yamaguchi, Y.; Gojobori, T.; et al. *Proc. Natl. Acad. Sci. U.S.A.* **1994**, *91*, 6269–6273.
- (73) Blagitko, N.; Schulz, U.; Schinzel, A. A.; Ropers, H. H.; Kalscheuer, V. M. *Hum. Mol. Genet.* **1999**, *8*, 2387–2396.
- (74) Verheijen, F. W.; Verbeek, E.; Aula, N.; Beerens, C. E.; Havelaar, A. C.; Joosse, M.; Peltonen, L.; Aula, P.; Galjaard, H.; van der Spek, P. J.; Mancini, G. M. *Nat. Genet.* **1999**, *23*, 462–465.
- (75) Kuvbachieva, A.; Bestel, A. M.; Tissir, F.; Maloum, I.; Guimiot, F.; Ramoz, N.; Bourgeois, F.; Moalic, J. M.; Goffinet, A. M.; Simonneau, M. *Eur. J. Neurosci.* **2004**, *20*, 603–610.
- (76) Kato, H.; Chen, S.; Kiyama, H.; Ikeda, K.; Kimura, N.; Nakashima, K.; Taga, T. *J. Biochem. (Tokyo)* **2000**, *128*, 923–932.
- (77) Farhang-Fallah, J.; Yin, X.; Trentin, G.; Cheng, A. M.; Rozakis-Adcock, M. *J. Biol. Chem.* **2000**, *275*, 40492–40497.
- (78) Bauer, P. H.; Muller, S.; Puzicha, M.; Pippig, S.; Obermaier, B.; Helmreich, E. J.; Lohse, M. *J. Nature* **1992**, *358*, 73–76.
- (79) Kambouris, M.; Triarhou, L. C.; Dlouhy, S. R.; Sangameswaran, L.; Luo, F.; Ghetti, B.; Hodes, M. E. *Brain Res. Mol. Brain Res.* **1994**, *25*, 183–191.
- (80) Ko, J. L.; Loh, H. H. *J. Neurochem.* **2005**, *93*, 749–761.
- (81) Haque, S. J.; Petersen, D. D.; Nebert, D. W.; Mackenzie, P. I. *DNA Cell Biol.* **1991**, *10*, 515–524.
- (82) Martinasevic, M. K.; King, C. D.; Rios, G. R.; Tephly, T. R. *Drug Metab. Dispos.* **1998**, *26*, 1039–1041.
- (83) Li, J.; Wang, Y.; Zhou, R.; Zhang, H.; Yang, L.; Wang, B.; Faraone, S. V. *Am. J. Med. Genet., Part B* **2006**, *141*, 126–129.
- (84) Sheehan, K.; Hawi, Z.; Gill, M.; Kent, L. *Neurosci. Lett.* **2007**, *412*, 105–107.
- (85) Shi, J. D.; Kukar, T.; Wang, C. Y.; Li, Q. Z.; Cruz, P. E.; Davoodi-Semiromi, A.; Yang, P.; Gu, Y.; Lian, W.; Wu, D. H.; She, J. X. *J. Biol. Chem.* **2001**, *276*, 17474–17478.
- (86) Suzuki, K.; Suzuki, Y. *Proc. Natl. Acad. Sci. U.S.A.* **1970**, *66*, 302–309.
- (87) Kondo, Y.; Wenger, D. A.; Gallo, V.; Duncan, I. D. *Proc. Natl. Acad. Sci. U.S.A.* **2005**, *102*, 18670–18675.
- (88) Lufei, C.; Ma, J.; Huang, G.; Zhang, T.; Novotny-Diermayr, V.; Ong, C. T.; Cao, X. *EMBO J.* **2003**, *22*, 1325–1335.
- (89) Voigt, P.; Dorner, M. B.; Schaefer, M. *J. Biol. Chem.* **2006**, *281*, 9977–9986.
- (90) Narita, M.; Imai, S.; Narita, M.; Kasukawa, A.; Yajima, Y.; Suzuki, T. *Neuroscience* **2004**, *124*, 515–521.
- (91) Baquet, Z. C.; Bickford, P. C.; Jones, K. R. *J. Neurosci.* **2005**, *25*, 6251–6259.
- (92) Mogi, M.; Togari, A.; Kondo, T.; Mizuno, Y.; Komure, O.; Kuno, S.; Ichinose, H.; Nagatsu, T. *Neurosci. Lett.* **1999**, *270*, 45–48.
- (93) Zuccato, C.; Ciammola, A.; Rigamonti, D.; Leavitt, B. R.; Goffredo, D.; Conti, L.; MacDonald, M. E.; Friedlander, R. M.; Silani, V.; Hayden, M. R.; Timmusk, T.; Sipione, S.; Cattaneo, E. *Science* **2001**, *293*, 493–498.
- (94) Watson, D.; Ando, T.; Knight, J. F. *Immunogenetics* **2000**, *51*, 714–722.
- (95) Hvas, J.; Oksenberg, J. R.; Fernando, R.; Steinman, L.; Bernard, C. C. *J. Neuroimmunol.* **1993**, *46*, 225–234.
- (96) Parker, M. G.; White, R.; Hurst, H.; Needham, M.; Tilly, R. *J. Biol. Chem.* **1983**, *258*, 12–15.
- (97) Bardoni, B.; Castets, M.; Huot, M. E.; Schenck, A.; Adinolfi, S.; Corbin, F.; Pastore, A.; Khandjian, E. W.; Mandel, J. L. *Hum. Mol. Genet.* **2003**, *12*, 1689–1698.
- (98) Reddi, P. P.; Flickinger, C. J.; Herr, J. C. *Biol. Reprod.* **1999**, *61*, 1256–1266.

### Model for ADHD Research

- (99) Zhang, H.; Jones, R.; Martin-DeLeon, P. A. *Matrix Biol.* **2004**, *22*, 653-661.
- (100) Dang, D. T.; Pevsner, J.; Yang, V. W. *Int. J. Biochem. Cell Biol.* **2000**, *32*, 1103-1121.
- (101) Chanchevalap, S.; Nandan, M. O.; Merlin, D.; Yang, V. W. *FEBS Lett.* **2004**, *578*, 99-105.
- (102) Maitra, R.; Grigoryev, D. N.; Bera, T. K.; Pastan, I. H.; Lee, B. *Biochem. Biophys. Res. Commun.* **2003**, *303*, 842-847.
- (103) Yue, Y.; Grossmann, B.; Holder, S. E.; Haaf, T. *Hum. Genet.* **2005**, *117*, 1-8.
- (104) Liu, L.; Chen, G.; Ji, X.; Gao, G. *Biochem. Biophys. Res. Commun.* **2004**, *321*, 517-523.

### research articles

- (105) Xia, X.; Hou, F.; Li, J.; Nie, H. *Biochem. Biophys. Res. Commun.* **2005**, *336*, 281-286.
- (106) Yoshimura, Y.; Shinkawa, T.; Taoka, M.; Kobayashi, K.; Isobe, T.; Yamauchi, T. *Biochem. Biophys. Res. Commun.* **2002**, *290*, 948-954.
- (107) Tang, G.; Ren, D.; Xin, R.; Qian, Y.; Wang, D.; Jiang, S. *Am. J. Med. Genet.* **2001**, *105*, 485-488.
- (108) Murphy, E. V.; Zhang, Y.; Zhu, W.; Biggs, J. *Gene* **1995**, *159*, 131-135.

PR800025T